Final Report

Contract # F4920-96-C-0005

Ultra-sensitive Laser Ionization Technique for Real-time Analysis-Control (ULTRA) of Silicon-MBE

Submitted by: SVT Associates, Inc.
7620 Executive Drive
Eden Prairie, MN 55344
Ph. (612) 934-2100 x-241
FAX (612) 934-2737
e-mail: svta@svta.com

Principal investigators: Dr. Peter Chow
Ph. (612) 934-1898
e-mail: pchow@svta.com
Dr. Jody Klaassen
Ph. (612) 934-2100 x247
e-mail: klaassen@svta.com

Subcontractors: Prof. Steve Leone, Univ. of Colorado
Prof. Kang Wang, Univ. of California, Los Angeles

REPORT DOCUMENTATION PAGE

AFRL-SR-BL-TR-99-
0215

1. AGENCY USE ONLY *(Leave blank)*	2. REPORT DATE	3. REPO
		01 Sep 98 to 31 May 99 Final

4. TITLE AND SUBTITLE
Ultra-Sensitive Laser-Ionization for Real-Time Analysis-Control (ULTRA) of Silicon-MBE

5. FUNDING NUMBERS
61101E
D178/05

6. AUTHOR(S)
Dr Chow

7. PERFORMING ORGANIZATION NAME(S) AND ADDRESS(ES)
SVT Associates Inc
7620 Executive Drive
Eden Prairie, MN 55344-3677

8. PERFORMING ORGANIZATION REPORT NUMBER

9. SPONSORING/MONITORING AGENCY NAME(S) AND ADDRESS(ES)
AFOSR/NE
801 North Randolph Street Rm 732
Arlington, VA 22203-1977

10. SPONSORING/MONITORING AGENCY REPORT NUMBER
F49620-96-C-0005

11. SUPPLEMENTARY NOTES

12a. DISTRIBUTION AVAILABILITY STATEMENT
APPROVAL FOR PUBLIC RELEASED; DISTRIBUTION UNLIMITED

12b. DISTRIBUTION CODE

The objective of the ultra-sensitive Laser-Ionization for Real-Time Analysis Control (ULTRA) program was to develop and advanced growth diagnostics instrument for molecular beam epitaxy (MBE) systems which will provide date during material deposition of growth species fluxes and epitaxial growth rate in the most non-intrusive manner possible.
This program was a cooperative "team" effort between SVT Associates and researchers at the University of Colorado, Boulder and the Univesity of Calfornia, Los Angeles.
In this report we will discuss the progress made in specific tasks outlined for this three year program. The highlights of this program are the following.
Optimized Ultra Tool by implementation of high quality laser and optics:
factor of five increase in 9th harmonic (118nm) generation;
low cost atomic resonance lamps examined as alternative VUV source;
optimization of Time-of-Flight (TOF) hardware;
quantification of the detection efficiency of flux species.
Implemented Sensor Suite for MBE Process:
implementation of prototype ULTRA on deposition systems;
development of optical scattering and advanced pyrometry tools;
interface-capability to process automation software control.
Developed Fabrication Process of Nano-structures:
surface dynamics study of GaAs homoepitaxy;
InAs quantum dot growth on GaAs;
SiGe nano-structure fabrication as function of flux and temperature;
investigation of the effect of surfactants.

17. SECURITY CLASSIFICATION OF REPORT	18. SECURITY CLASSIFICATION OF THIS PAGE	19. SECURITY CLASSIFICATION OF ABSTRACT	20. LIMITATION OF ABSTRACT
UNCLASSIFIED	UNCLASSIFIED	UNCLASSIFIED	UL

Table of Contents

I. Executive Summary:

The objective of the **U**ltra-sensitive **L**aser-Ionization for **R**eal-Time **A**nalysis-Control (ULTRA) program is to develop an advanced growth diagnostics instrument for molecular beam epitaxy (MBE) systems which will provide data during material deposition on growth species fluxes and epitaxial growth rate in the most non-intrusive manner possible. MBE offers the possibility for the most stringent control of growth conditions, control which is necessary for the every increasing demands on dimensional and compositional tolerances required in advanced semiconductor technology. Diagnostic techniques such as ULTRA are an important research direction which provides not only new tools necessary for the engineering of advanced semiconductor devices, but also an increased understanding of the fundamental science, the chemistry and physics, underlying the development of these devices.

This program is a cooperative "team" effort between SVT Associates and researchers at the University of Colorado, Boulder and the University of California, Los Angeles. Prof. Steve Leone of the Department of Chemistry at the University of Colorado is the inventor of the single photon ionization - time of flight mass spec technique. His group has been refining this technique while studying basic surface kinetics and dynamics involved in the growth of gallium arsenide films. Prof. Kang Wang of the Electrical Engineering Department at UCLA is an expert in the growth of group IV nanostructures and quantum devices. Professor Kang's group provided a MBE test site, designed and built by SVTA, which is capable of implementing the ULTRA sensor and utilizing it in the growth of silicon nanostructures. There was also significant interaction with Professor Mohan Krishnamurphy of the Michigan Technology University on SiGe quantum structure fabrication. The combination of SVTA's experience in MBE hardware technology with the fundamental science expertise of the university groups has made this development program a successful one.

Key Accomplishments:

In this report we will discuss the progress made in specific tasks outlined for this three year program. The highlights of this program are the following.

Optimized Ultra Tool By implementation of high quality laser and optics

- Factor of five increase in 9th harmonic (118 nm) generation
- Low cost atomic resonance lamps examined as alternative VUV source

- Optimization of Time-of-Flight (TOF) hardware
- Quantification of the detection efficiency of flux species

Implemented Sensor Suite for MBE Process

- Implementation of prototype ULTRA on deposition system
- Development of optical scattering and advanced pyrometry tools
- Interface-capability to process automation software control

DevelopedFabrication Process of Nano-structures

- Surface dynamics study of GaAs homoepitaxy
- InAs quantum dot growth on GaAs
- SiGe nano-strucutre fabrication as function of flux and temperature
- Investigation of the effect of surfactants

II. Project overview:

A schematic overview of the prototype ULTRA sensor is shown in Figure II-1. This system has been developed in Prof. Steve Leone's group at the University of Colorado. The ULTRA sensor combines a time-of-flight (TOF) mass spectrometer using VUV light as a photoionization source with reflection high energy electron diffraction (RHEED) in order to monitor both the fluxes of gas phase growth species and growth rate and surface condition during MBE material deposition. The ionizing VUV radiation is generated from the 9th harmonic (118 nm) of a Nd:YAG laser. In the prototype system at the University of Colorado, the TOF mass spectrometer is arranged to sample fluxes depositing onto and desorbing from the surface of a small (<1 inch) substrate. In this fundamental research prototype system, the beam fluxes are spatially very well defined. It is possible in this system to steer the 118 nm ionizing light to probe primarily just the incident flux onto the substrate or to probe flux which consists primarily of scattered and desorbing species from the growth surface. This ability to distinguish between incident and scattered flux allows the group at the University of Colorado to perform unique experiments on the kinetics and dynamics of epitaxial material growth. While there are significant differences between the research oriented prototype ULTRA system at the University of Colorado and commercial MBE systems, the ability to distinguish incident and scattered flux is a large part of what makes developing this technique an attractive commercialization project.

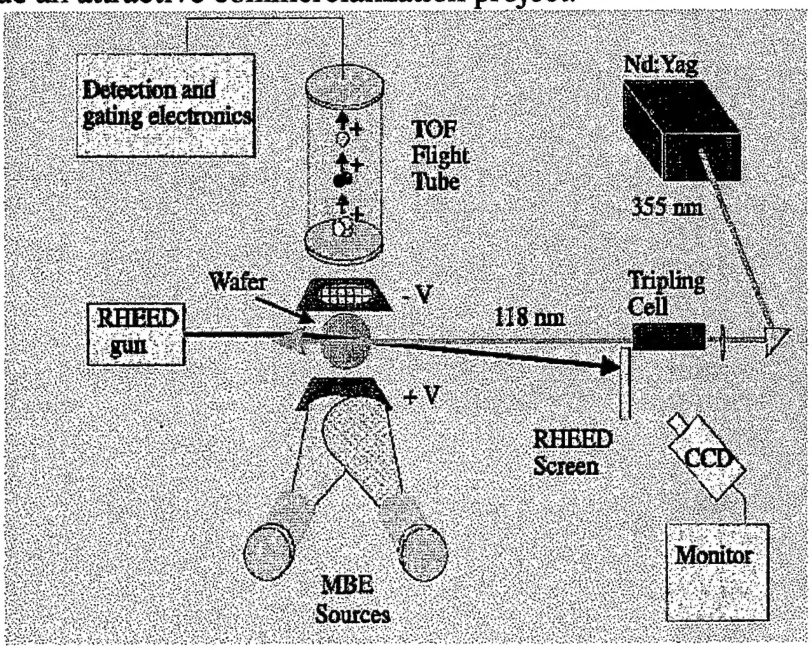

Figure II.1. A schematic overview of the prototype ULTRA system.

This report will describe the progress made and difficulties encountered in program to refine and further develop the ULTRA sensor technique for a commercial product for Si-MBE.

1. Design and implementation of high quality laser and optics

One of the most important aspects of the ULTRA sensor is the VUV light source used to photoionize, but not fragment, flux species used during MBE material growth. Photoionization instead of electron impact ionization allows for the selective detection of growth and dopant species over background gases in the system. For example, an important dopant in III-V material systems is silicon, atomic mass 28. Nitrogen, N_2 and carbon monoxide, CO, two common background gases in MBE systems, are also mass 28. But since silicon has an ionization potential (IP) of lower than the energy of the ionizing radiation while N2 and CO have IPs greater than the ionizing radiation silicon is selectively ionized and detected in the presence of these background gases.

Two very different VUV light sources are being investigated for suitability in a commercial instrument. The first source, and the one currently implemented on the ULTRA prototype, is generation of the ninth harmonic of Nd:YAG at 118 nm by first frequency tripling the Nd:YAG fundamental (1064 nm) in a nonlinear optical crystal (BBO or KDP) to create the UV third harmonic at 355 nm and then again tripling the third harmonic in gas mixtures of xenon and krypton to create the ninth harmonic at 118 nm. The second VUV source under investigation is an older technology, more of "low-tech" approach. It is the use of atomic resonance lines from a microwave discharge lamp to generate continuous, bright VUV radiation. The unique features of these two VUV systems, their advantages and disadvantages are summarized in Table II.1 below and discussed in the following section.

Table 1. Comparison of VUV Generation by 9th Harmonic of Nd:YAG and by Microwave Discharge Resonance Lamp

9th Harmonic of Nd:YAG	Microwave Discharge Lamp
118 nm	107, 117, 122, 124 nm
pulsed source	continuous source
low rep. rate (100 Hz)	high rep. rate (10,000 Hz) with pulsed extraction plates
high pulse fluence (10^{11}/pulse)	low pulse fluence (~10^{8}/pulse)
high cost ~ $100,000	low cost ~ $10,000

The 9th harmonic of Nd:YAG technique of VUV generation has several inherent advantages for an ionizing light source. It is laser generated light which can be well collimated and focused. The laser pulse is very short, <10 ns, and has high pulse energy, >100 nJ/pulse or >10^{11} photons/pulse. Short pulse length and high pulse fluence are ideal for a TOF ionization source. The disadvantages of 9th harmonic generation of Nd:YAG for an ionizing light source lie primarily in the expense, size, and complexity of the laser system. The laser in use on the prototype system is an excellent high-end research tool with exceptional performance. It is also very expensive, ~$100,000, occupies a large footprint, 4' x 8' minimum, and, being designed as a research tool, is not a turnkey system capable of assuring 99% up time.

Microwave Resonance Lamps

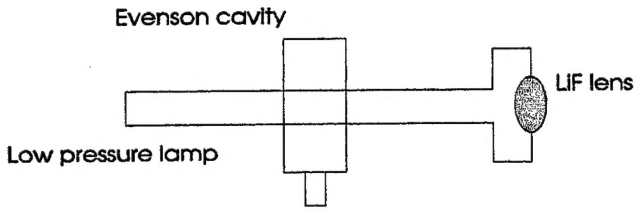

VUV resonance lines

Gas	Wavelength	Output (photons/s)
Ar	106.7 nm	------
Kr	116.5, 123.6 nm	10^{15}
H	121.6 nm	10^{14}

Figure II.2. The VUV lines and output powers of several gases typical in microwave discharge lamps.

Generation of VUV light with a microwave plasma resonance lamp source has several disadvantages compared to the 9th harmonic generation technique, but the technique also has a number of strong points which may make it a viable alternative for a commercial instrument. The primary advantages of a VUV resonance lamp as an photoionizing source are its low cost, small size, and simplicity of operation. A complete resonance lamp setup with lamp, microwave resonance cavity and microwave power supply is accessible for less than $10,000. The microwave power supply is rack mountable and the lamp itself is small enough to mount directly on a UHV flange. The major drawback with this system as compared with 9th harmonic generation is in the usability of the VUV light which is generated. Microwave lamp sources can be quite bright, but as incoherent sources they lack the directional capabilities of a laser source. Light collection, collimation and focusing, are more difficult than with laser sources. Also, the microwave resonance lamp is a continuous light source. This can be advantageous in a TOF system since the repetition rate for sending ions up the drift tube is determined by pulsing the extraction plates rather than by pulsing the laser. Repetition rates of 10 kHz are quite feasible in contrast to only 100 Hz for a high performance pulsed laser.

2. Optimization of Time-of-Flight (TOF) hardware

One of the important tasks accomplished during the first year of this program is the optimization of the mass spectral signals from the ULTRA sensor and an evaluation of what elements of the system must be improved or modified. Use of a new state-of-the-art Nd:YAG laser (Coherent, Infinity model) having an order of magnitude higher repetition rate (100 Hz), narrower line width, better pulse stability and an improved spatial beam profile has made a significant improvement. The higher repetition rate of 100 Hz allowed for better signal averaging and greater time resolution for measurement of fast kinetic changes. The high quality beam shape and other laser characteristics such as narrow linewidth and good stability of pulse energy allowed for a factor of five improvement in the frequency tripling

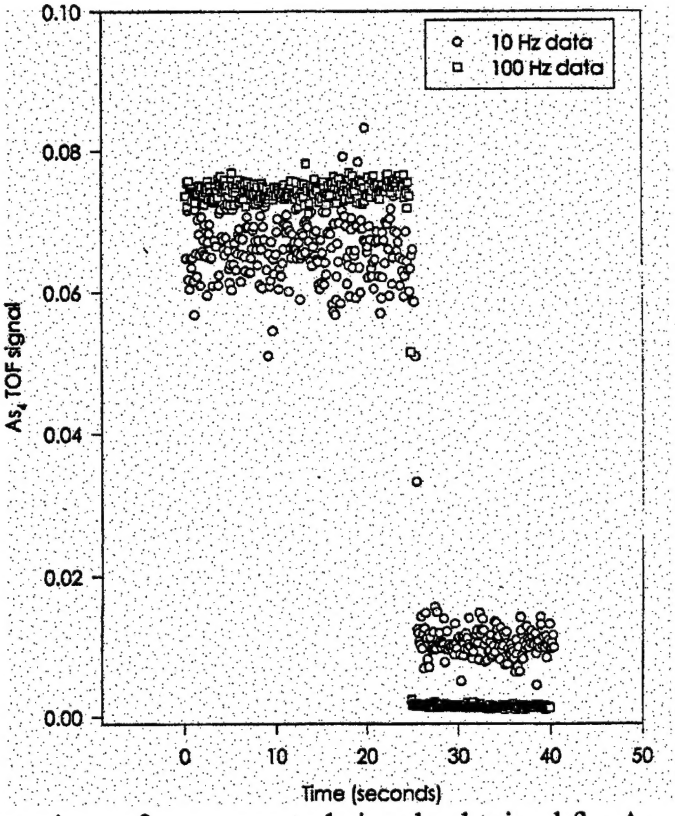

Figure II.3. Comparison of mass spectral signals obtained for As_4 using a new high-performance 100 Hz laser with older data taken with a less sophisticated 10 Hz laser.

conversion of 355 nm photons to 118 nm photons. Optics in the tripling cell region were improved. A large 1" diameter UHV compatible LiF window allowed for greater beam steering so that incident photons could intersect only scattered arsenic and gallium molecules from the surface or the beam could be adjusted to intersect some portion of both scattered and incident molecular beams of As_4 and Ga.

The ion detection equipment is an important part of the TOF mass spec design. Particularly in arsenic and antimonide systems where the corrosive nature of these materials precludes use of delicate, high sensitivity multichannel plates (MCPs). A regenerated electron multiplier was installed in the TOF to provide additional improvement in the signal-to-noise ratio of mass signals for the system with the new laser compared with the older laser system. Figure II.3 demonstrates the overall improvement achieved by the installation of the new laser and regenerated detector compared to previously obtained data. The As_4 mass signal obtained for the new data was collected at 100 Hz and every 10 points were averaged. The As_4 mass signal shown from the previous data was collected at 10 Hz and was not signal averaged. The fluxes of As_4 were comparable in both cases. The arsenic oven shutter was closed at 25 seconds. The reduction in the scatter in the data for the new system can clearly be seen.

The improved ULTRA prototype was used to study arsenic incorporation during GaAs homoepitaxy as a function of both incident Ga flux and substrate temperature. While the trends in the results matched those obtained prior to the experimental improvements, the scatter in the data decreased markedly. Figure II.4 shows the steady-state decrease in As_4 as a function of Ga TOF signal (proportional to incident Ga flux) before and after the experimental changes. The newer data show the leveling out of the steady-state decrease in As_4 at higher gallium fluxes much better than the older data. Further, the alignment of the laser in a position to intersect all scattered molecules from the GaAs wafer has allowed observation of scattered gallium atoms from the heated GaAs wafer.

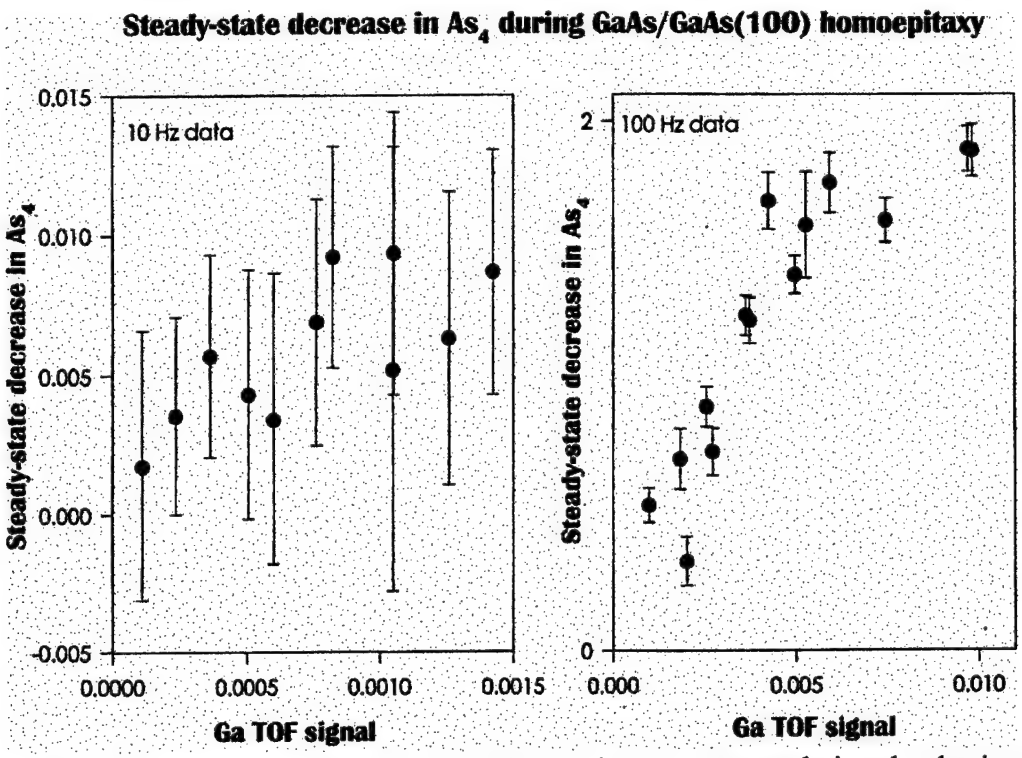

Figure II.4. Comparison of steady state change in mass spectral signals obtained for As_4 as a function of the Ga mass spec signal using a new high-performance 100 Hz laser with older data taken with a less sophisticated 10 Hz laser.

Desorption kinetics of As_2 from GaAs(100) and Si(100) were also measured using the ULTRA sensor. The time resolution of the new laser along with the improvements in signal-to-noise ratio provided the capability to fit the rate of loss of arsenic coverage from the surface as a function of time. This information along with the measurement of steady-state fluxes of arsenic desorbing from the wafer give a picture of the surface chemistry of arsenic interactions on the surfaces studied.

3. Quantification of the detection efficiency of flux species

Most of the work with the prototype ULTRA sensor has been on GaAs homoepitaxy. In this part of the project we are beginning to apply the ULTRA sensor to other material systems, in particular silicon/germanium heteroepitaxy, to quantify the detection efficiency of the ULTRA sensor for these systems, and to utilize ULTRA for fundamental studies of surface chemistry kinetics and dynamics. Progress has been made on the study of arsenic interactions with both the Si(100) and Ge(100) surfaces. These studies are relevant to many important issues in Group IV epitaxy, such as dopant incorporation during growth and surfactant-enhanced epitaxy, as well as being important for GaAs growth on both Si and Ge.

Figure II.5 shows the mass spectral signals arising from species scattered and desorbing from a Si(100) surface [p-type, 10-20 Ωcm resistivity] heated under an incident As_4 flux. As the surface temperature is raised above ~700 °K the incident As_4 beam undergoes a cracking reaction on the surface to produce As_2. The amount of As_2 produced increases fairly steadily with increasing surface temperature from ~675 °K up to ~ 875 °K and then begins to level off. The increase and leveling off in As_2 is mirrored by a corresponding decrease and

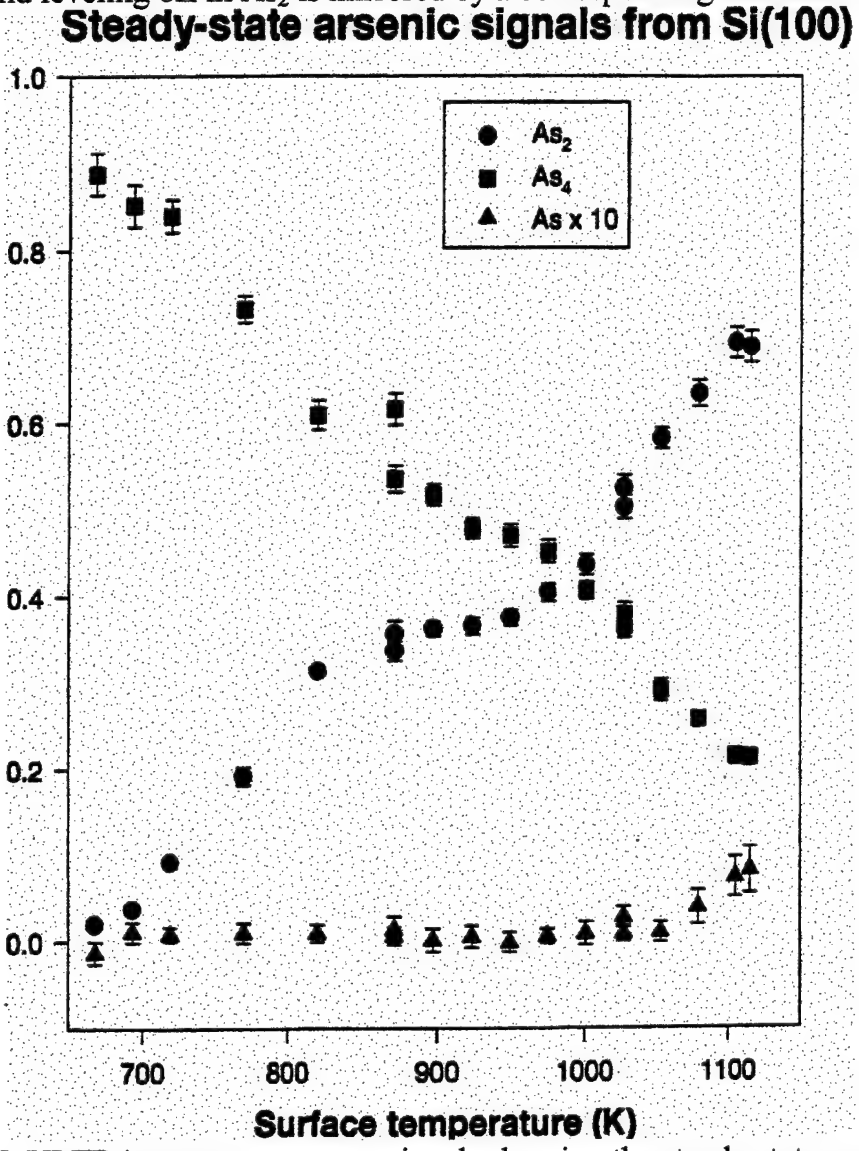

Figure II.5. ULTRA sensor mass spec signals showing the steady state scattered arsenic flux from Si(100) substrate as a function of surface temperature.

leveling off in the amount of As_4 produced. The leveling off in both signals is maintained until ~975 °K. Above this temperature, the As_2 signal again starts to rise while the As_4 signal decreases. The As_2 signal continues to rise until ~1100

°K. At 1075 °K an As atom desorption channel is observed, the atom signal increasing with increasing surface temperature.

The mass spectral signal levels from the ULTRA probe can be directly related to the fluxes of gas phase species to and from the substrate. For the data shown in Figure II.5, the ULTRA probe is intersecting only species scattered and/or desorbing from the substrate, thus the signal levels can be related to fluxes of species leaving the surface. This allows kinetic measurements involving the outgoing fluxes of these species to be made. An example is shown in Figure II.6

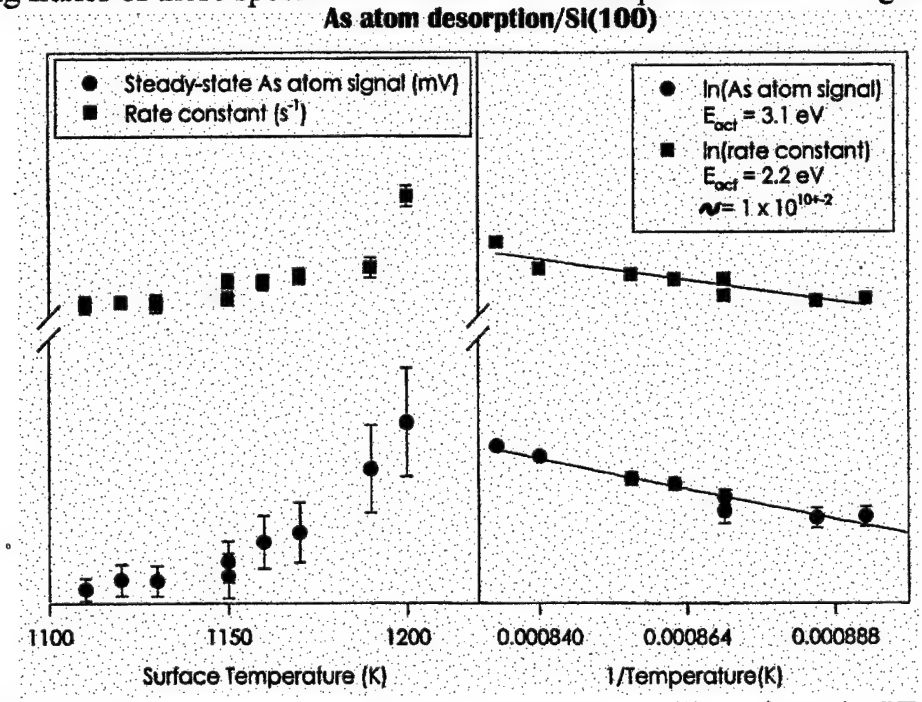

Figure II.6. Kinetic data for arsenic atom formation on silicon from the ULTRA sensor probing only scattered and desorbing flux.

for the atomic arsenic species. The left hand side of this figure shows the arsenic atom signal level (circles) as a function of the surface temperature. Additionally this plot shows the atom desoption rate constants (squares), also plotted as a function of surface temperature (the y-axes of the plots shown in the figure are given in relative units to facilitate this comparison). The rate constant is obtained by fitting the decay rate of the atomic signal after the oven shutter is closed. Arrhenius plots can be constructed for both of these data sets, and these are shown in the right-hand side of Figure II.6. The slopes of these lines give the activation energy for the desorption of arsenic atom from the Si(100) surface. Using the signal level measurements (circles), an activation energy of 3.1 eV is obtained and using the rate constants derived from the decay times, an activation energy of 2.2 eV is obtained (squares). A pre-exponential factor of $1x10^{10\pm2}$ s-1 for the desorption process is obtained. When this treatment is applied to the As_2

desorption channel, non-Arrhenius behavior is observed. Work is continuing on the interpretation of the As_2 desorption data and also on reconciling the activation energies for As atom desorption from silicon obtained by the two different methods.

Preliminary arsenic desorption studies have also carried out for Ge(100) surfaces [n-type, 0.3 Ωcm resistivity]. Figure II.7 shows kinetic plots for the germanium surface similar to those shown in Figure II.5 for silicon. The scattered As_4 is again observed to decrease upon elevation of the sample temperature, and a corresponding increase is seen in As_2. At elevated temperatures, ≥1000 °K, an atomic arsenic desorption channel is again observed to open. Further work must be carried out before quantitative kinetic parameters will be obtained for this system.

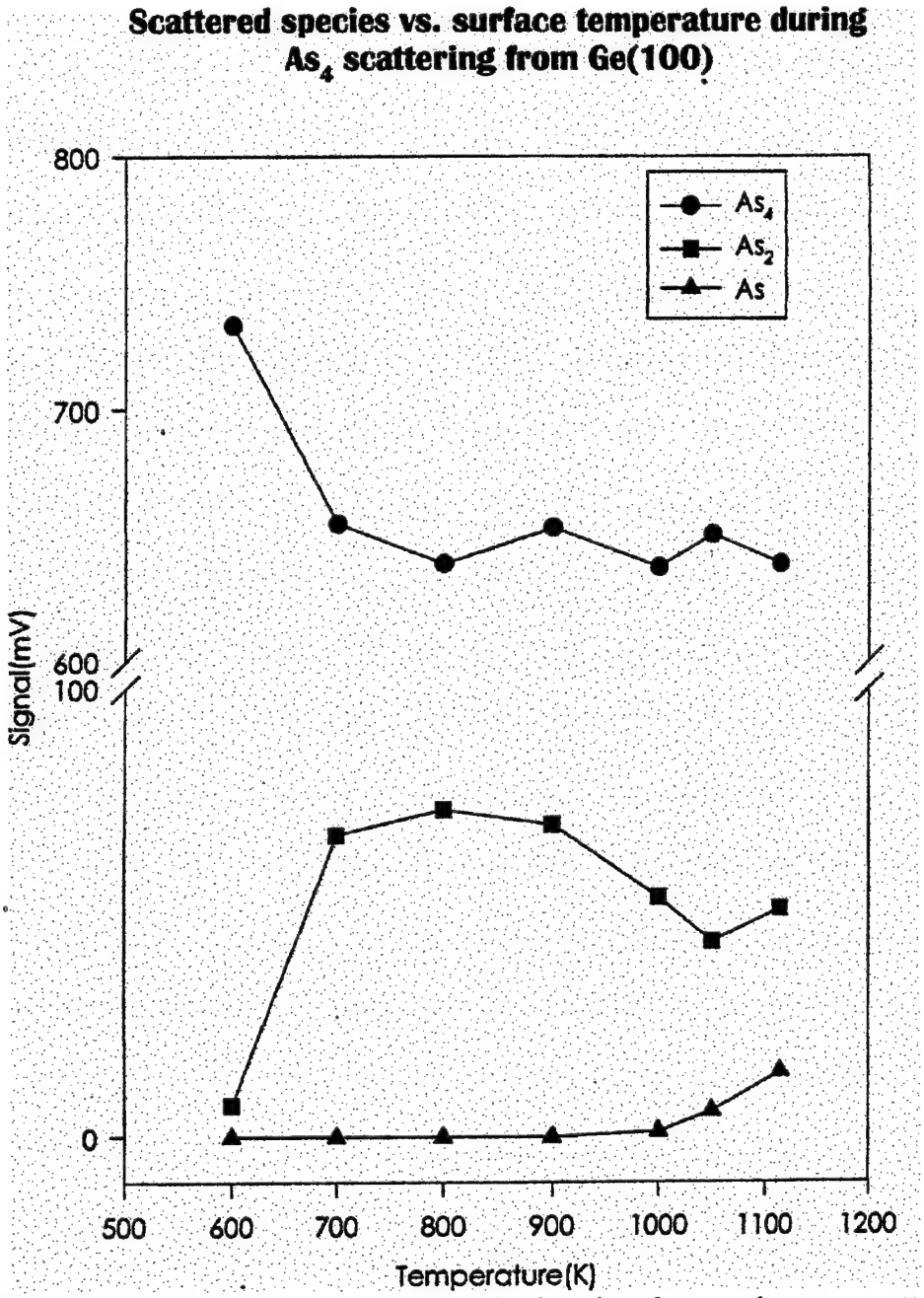

Figure II.7. ULTRA sensor mass spec signals showing the steady state scattered arsenic flux from Ge(100) substrate as a function of surface temperature.

4. Implementation of prototype ULTRA on deposition system

Currently the prototype ULTRA system is at the University of Colorado. The implementation of a similar system has yet to be done at SVT Associates. The reason for delay is related to moving from a fundamental research oriented tool for studying surface kinetics and dynamics, which is what the system at the

University of Colorado is, to a tool which will be applicable to commercial MBE systems devoted to producing materials for devices. We have been addressing issues such as how to incorporate the TOF design into an MBE system in such a way as to not shadow the substrate from the sources. One novel design under consideration is to use the substrate block itself as part of the extraction region in the TOF. For example, in the gas source silicon MBE system shown below we use a specially substrate block as the bottom extraction plate of the TOF mass spec. This would allow the ion acceleration plates and drift tube to in an ideal position perpendicular to the growth surface. Also, the main body of the TOF would be shielded behind the cryopanels of the MBE system. This arrangement of the TOF also allows for the possibility to distinguish between incident and desorbing flux by using delayed pulse extraction techniques. It may be possible to separate same mass species by whether their velocity vectors are parallel or anti-parallel to the ion extraction field.

A system incorporating an ULTRA sensor with its TOF perpendicular to the substrate is shown in Figure II.8. This figure is a sketch of an idealized system for Prof. Wang which would incorporate the ULTRA flux monitor with surface sensitive monitors such as RHEED and pyrometric interferometry (PI). These monitoring techniques, particularly the combination of ULTRA and PI will be used to develop real time analysis and control of MBE material growth, an ultimate objective of the ULTRA program.

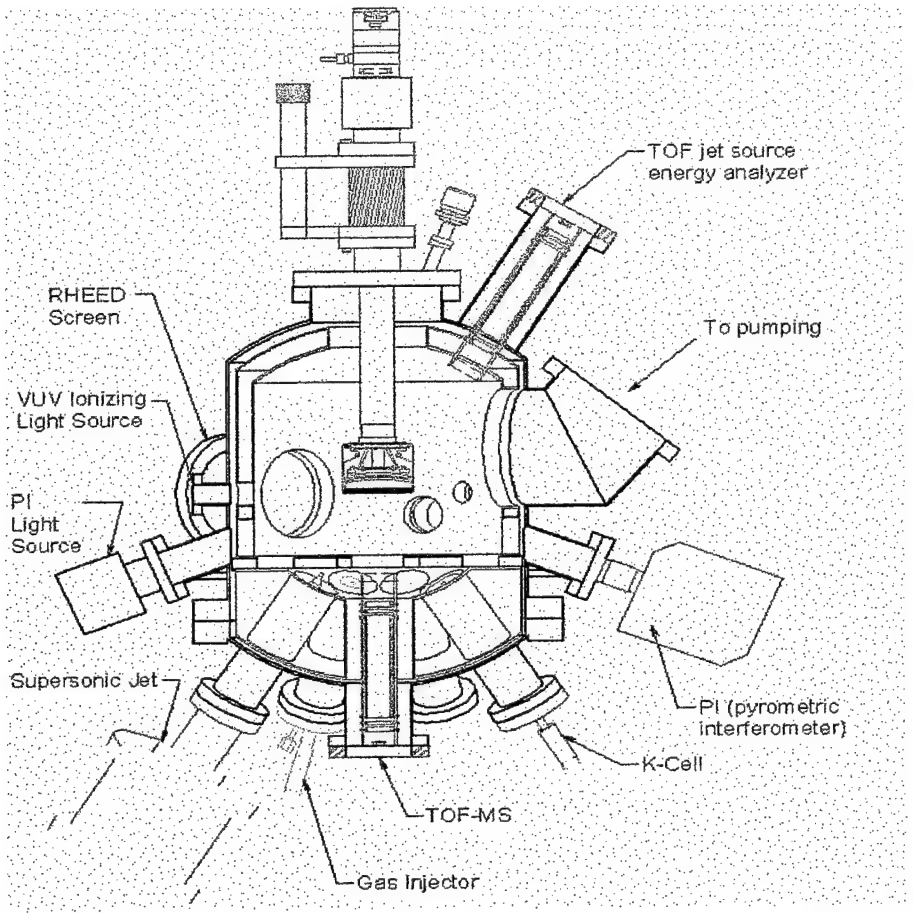

Figure II.8. Schematic drawing of an MBE system incorporating an ULTRA sensor perpendicular to the substrate and other surface sensitive monitoring techniques such as PI and RHEED.

5. Monitor Tool Set of Ultra in Combination with Other Techniques (RHEED, Optical Scatter and Pyrometry Instruments)

In order to ultimately address issues related to the fabrication of nanoscale devices, we have undertaken some preliminary studies on the growth self-assembled quantum dots of InAs on GaAs. The ULTRA sensor, with its sensitivity to flux incident and scattered from a growth surface may have a significant impact on understanding the kinetics and surface dynamics of quantum dot formation. It may be possible to see changes in flux incorporation with the ULTRA sensor when growth switches from 2-dimensional to 3-dimensional. Also, the growth of quantum dot structures has allowed us to investigate other techniques such as laser light scattering which are related to determination of substrate surface quality and epi-readiness.

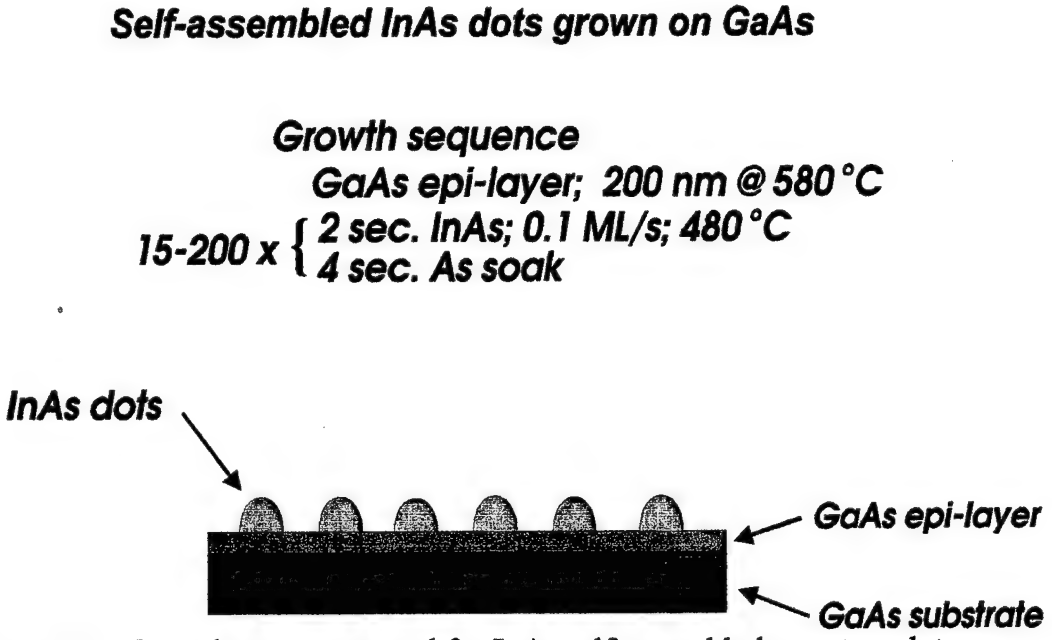

Figure II.9. Growth sequence used for InAs self-assembled quantum dots on GaAs.

InAs quantum dots were grown using the techniques and conditions reported in the literature. The growth sequence was carried out using an alternating shutter cycle, Figure II.9, which allowed for 2 seconds of InAs growth followed by 4 seconds of arsenic soak. The number shutter cycles was varied between 15 and 200 to put down between 2 and 20 equivalent monolayers of InAs.

The growth of the InAs self-assembled quantum dots was followed in situ by monitoring the changes in the RHEED pattern and its intensity. Figure II.10

shows a video capture of the 4-fold RHEED pattern observed for the GaAs epi-surface before InAs quantum dot formation and the hexagonal pattern of transmission spots observed after the surface goes to 3-dimensional islands.

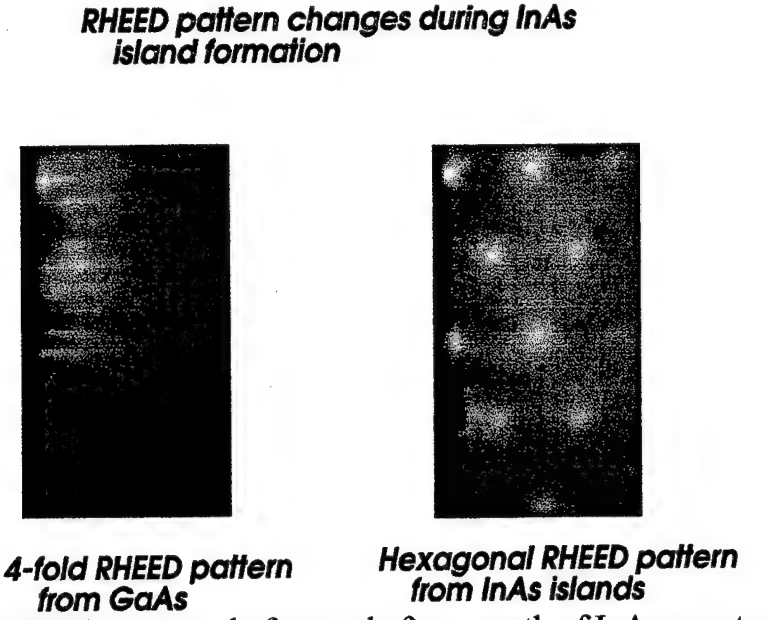

Figure II.10. RHEED patterns before and after growth of InAs quantum dots.

The intensity of the specular RHEED beam was also monitored during the initial phase of quantum dot growth as shown in Figure II.11. The shutter sequence of InAs growth followed by As anneal can be seen in the periodic changes in the RHEED intensity for approximately the first 1.5 monolayers of InAs deposition. After this amount of deposition, at ~60 seconds in Figure II.11, growth goes 3-dimensional and only a monotonic decrease in RHEED intensity is observed.

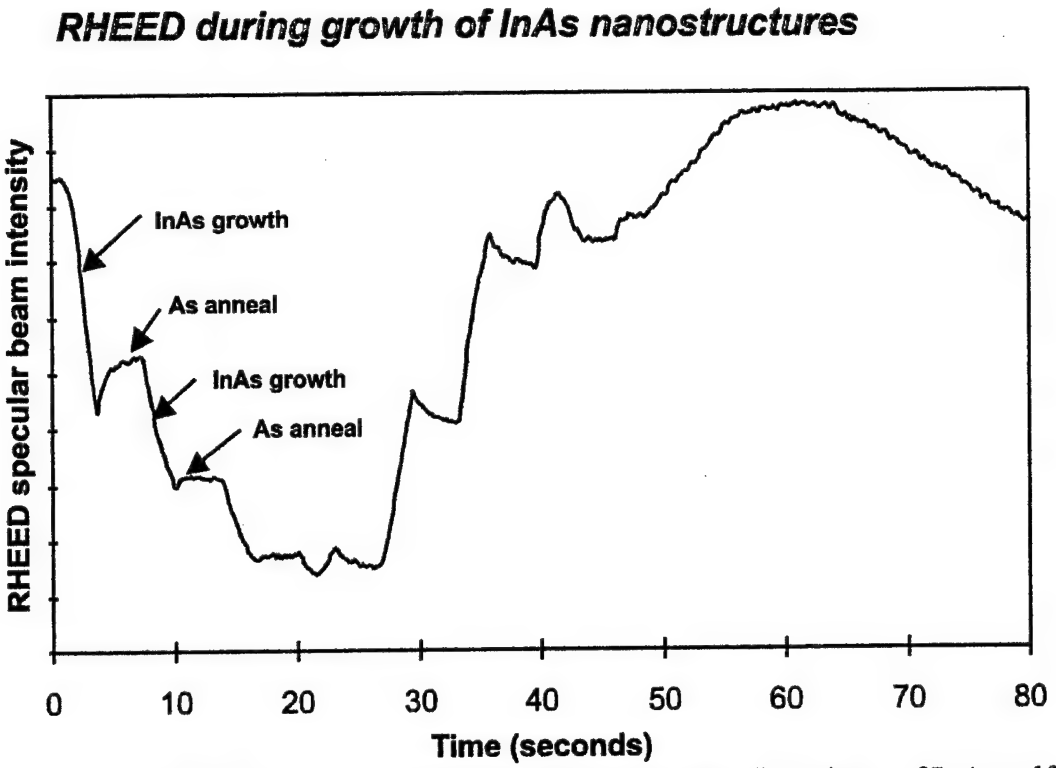

Figure II.11. RHEED specular beam intensity during the first phase of InAs self-assembled quantum dot growth on GaAs.

The InAs quantum dots were examined using both scanning electron microscopy (SEM) and atomic force microscopy (AFM). Figure II.12 shows a collage of SEM images for InAs quantum dots grown for 2, 5, 10, and 20 equivalent monolayers. The density of quantum dots is relatively constant at ~2.0 x 10^9 cm^{-2} for all four deposition levels. The mean lateral size of the dots, however, increases with the deposition level. AFM images and line scans for 2 equivalent monolayers and 20 equivalent monolayers of InAs are shown in Figures II.13 and II.14, respectively.

SEM Images of Self-assembled InAs nanostructures

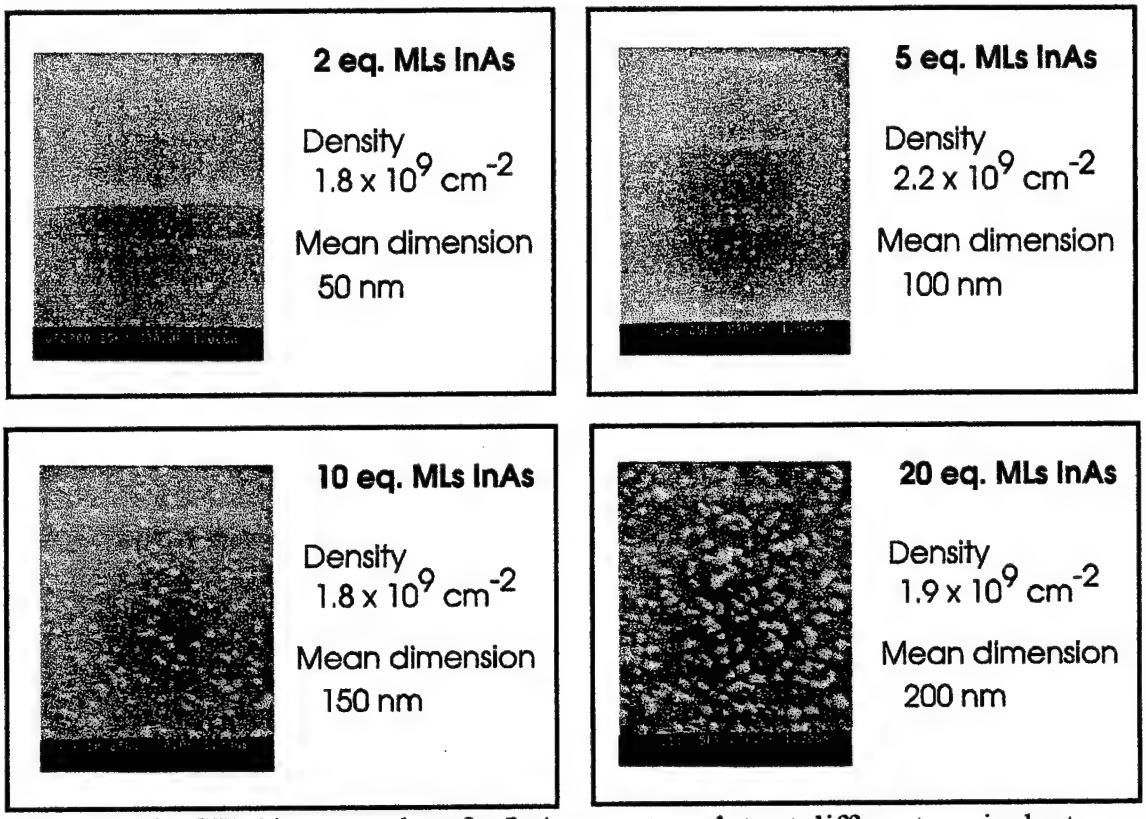

Figure II.12. SEM images taken for InAs quantum dots at different equivalent monolayers of InAs deposition.

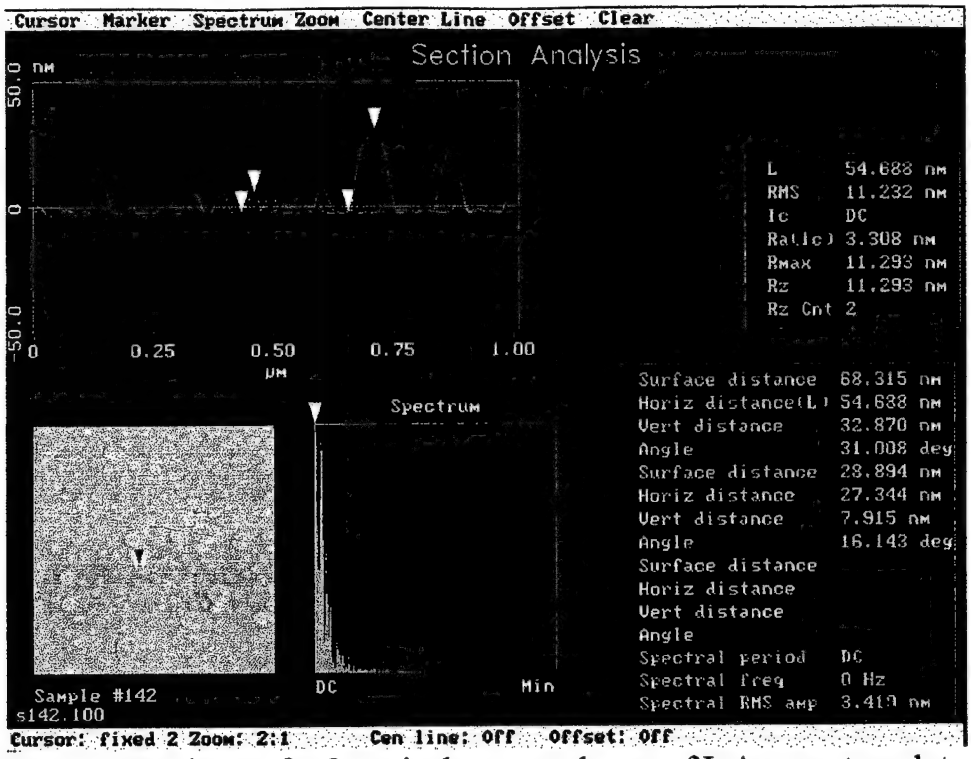

Figure II.13. AFM image for 2 equivalent monolayers of InAs quantum dot growth.

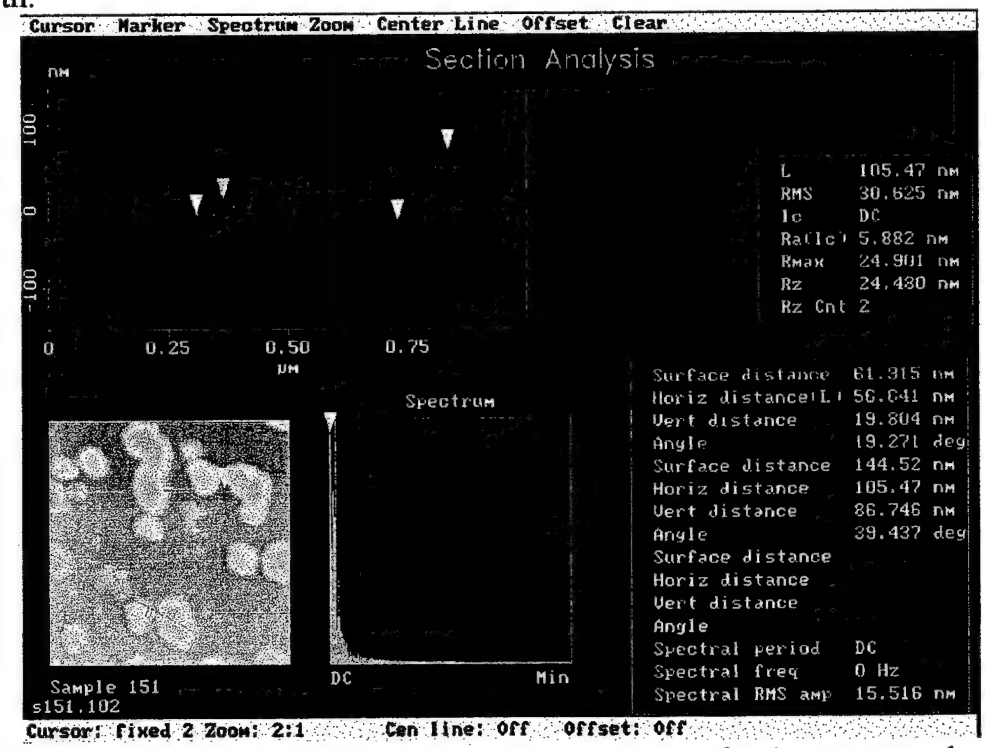

Figure II.14. AFM image for 20 equivalent monolayers of InAs quantum dot growth.

The AFM and SEM images of the InAs quantum dots show that the mean dimensions of the dots vary from ~50 to ~200 nm for 2 to 20 equivalent monolayers of growth. These are nanoscale dimensions. The 3-dimensional nature of the quantum dots precludes the use of RHEED to monitor their growth. We have investigated laser light scattering as a technique for monitoring the growth of nanoscale structures. The light scattering experiments were done ex situ on the benchtop, Figure II.15. A HeNe laser, 632.8 nm, modulated by a mechanical chopper was used as the light source. Scattered light was measured at a small angle, 15°, to the incident beam with a photomultiplier equipped with a bandpass filter for the HeNe light.

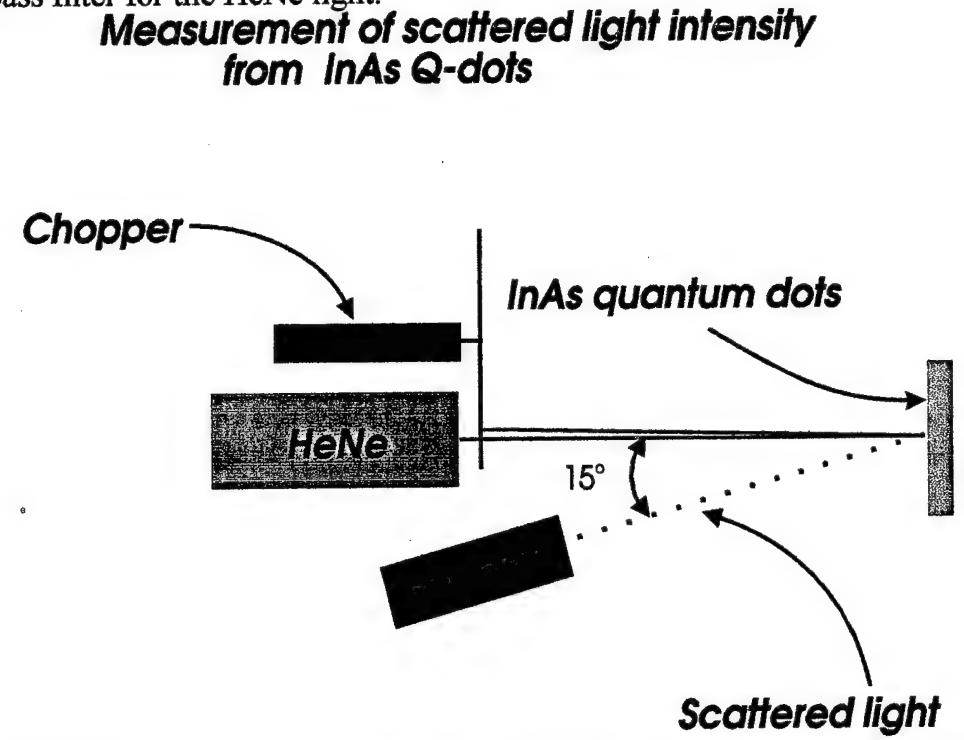

Figure II.15. Experimental arrangement for benchtop light scattering experiments with different sizes of InAs quantum dots.

The scattered light intensity was measured as a function of the number of equivalent monolayers InAs growth. The scattered light intensity was found to depend exponentially on number of equivalent monolayers of InAs deposition, Figure 16.

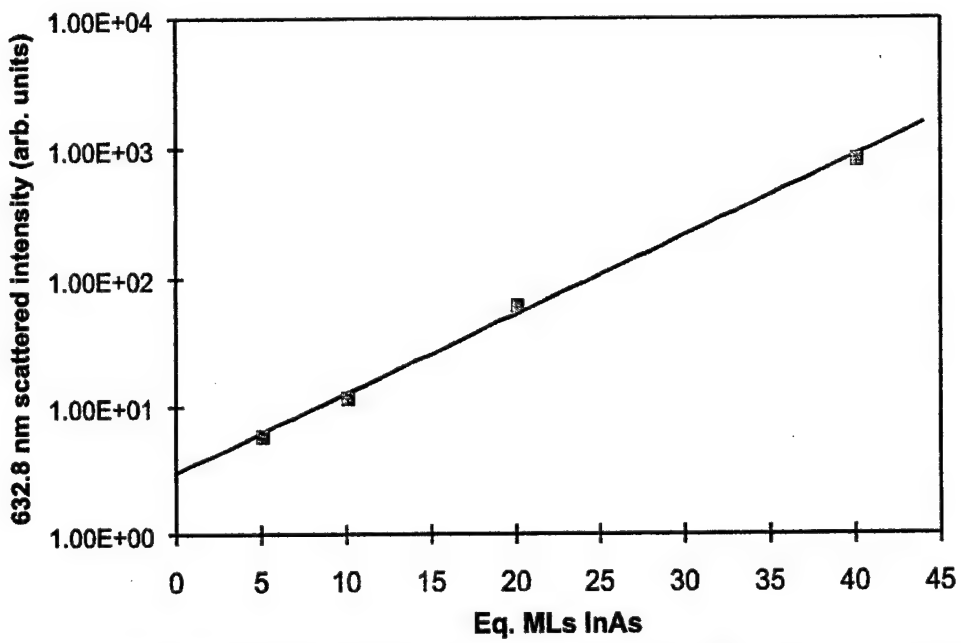

Figure II.16. Scattered light intensity increases exponentially with equivalent monolayers of InAs.

Interferometer Pyrometry (Model In-Situ 4000)

Pyrometry is a well established measurement technique and is successfully used in many applications. It has one main feature which makes it attractive for substrate temperature measurement during MBE or MOCVD: non-contact, vacuum compatible temperature sensing. At present most of nano-structure fabrication techniques are highly sensitive to the temperature parameter making close control very difficult. As those who have used pyrometry for semiconductor applications know, this technique has severe problems which greatly limit its usefulness. Some of those problems are summarized below.

-Substrate transparency
-Bandgap shifts.
-Viewport coating
-Obscuration errors
-Pickup of stray light
-Interference effects

-Film absorption effects

SVT Associates has recognized these difficulties and has, in conjunction with our own MBE processing lab and UHV system and components expertise, designed a new pyrometer system which solves many of the problems preventing pyrometry from becoming an indispensable tool for both MBE and MOCVD processes. This system combines traditional pyrometry with specular reflectometry to provide a single instrument to monitor both substrate temperature and film thickness in real time.

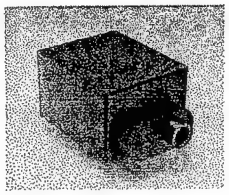

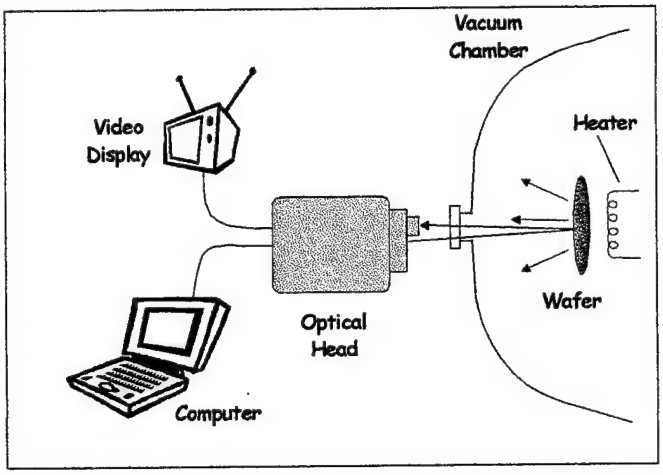

The schematic diagram above shows the layout of the In-Situ 4000 system. The integrated optical head contains the reflectometer illumination source, computer communications interface, and a video camera for ease of aiming and alignment with the substrate.

Solving Substrate Transparency

The problem of low emissivity and substrate transparency at infrared wavelengths is addressed by careful selection of the pyrometry wavelength. The In-Situ 4000 performs single wavelength pyrometry at 950 nm which is short enough to ensure that the substrate is opaque, and long enough to ensure a measurable optical radiation. Ensuring substrate opacity is a key element in addressing several of the previously listed difficulties. An opaque substrate prevents radiation from a filament heater from being transmitted though to the pyrometer. It also prevents other radiation sources in the chamber (effusion cells, ion gauge filaments, etc.) from scattering their light from the rough back side of the substrate into the

pyrometer. Since optical absorption and radiation are closely coupled, substrate opacity ensures that the emissivity of the substrate is high enough to provide a measurable signal. Typical substrates such as silicon, GaAs and InP are sufficiently opaque at 950 nm for substrate temperatures typical of epitaxial growth.

Solving Window Coating Problems

The problem of viewport window coating and optical alignment errors is addressed in the In-Situ 4000 through the use of "two-color" or "ratio" pyrometry which measures optical radiation at two wavelengths and takes the ratio of the measured intensities. If the pyrometer is well designed and the film coating the viewport is spectrally neutral, then the temperature may still be calculated since these errors affect both channels equally. Since many of the viewport coating problems deal with "metallic" type films (e.g. Ga, In, As), these films attenuate the light equally between the two wavelengths, the ratio calculation is still valid. If the viewport becomes coated with a dielectric film causing interference effects, then the ratio measurement becomes imbalanced and may not be valid.

The intensity ratio vs. substrate temperature will differ for varying substrate materials, so the In-Situ 4000 system allows the flexibility of a look-up table to translate from intensity ratio to reported temperature. This look-up table can be changed for different substrates, or updated to compensate for any calibration errors or instrument drift. The ratio pyrometry feature of the In-Situ 4000 provides the user with a repeatable day-to-day calibration which is independent of viewport coating effects.

Solving Varying Emissivity

The problem of unknown or shifting emissivity is solved using information from the accompanying reflectometer system. Under the conditions of an opaque substrate, a perfectly specular substrate front surface, and perfect uniformity of the deposited films, the emissivity may be measured via reflectometry at the same wavelength as the pyrometry. The relation linking emissivity, ε, and reflectometry, R, under these conditions is: $\varepsilon = 1 - R$. The In-Situ 4000 provides a 950 nm reflectometer which is matched to the 950 nm pyrometry system thus allowing this "emissivity compensation" to provide an emissivity independent temperature measurement. Thus, if the film being deposited has a index of refraction as the substrate producing interference effects, the reflectometry will observe these changes and the software will correct the error in the temperature calculation. The success of this technique depends upon how closely the materials system conform to the assumptions listed above, namely substrate opacity, surface

specularity (smoothness), and film uniformity. If the substrate is not sufficiently opaque or the surface is rough and scatters significant amount of light, the $\varepsilon = 1 - R$ relation is no longer true. If the deposited film is not uniform, then the reflectance measurement (made at a single point on the substrate) may not be well correlated to the pyrometry measurement (made over a large area of the substrate).

The figure below shows the temperature error which can occur when depositing multilayer thin films. The graph shows the measured substrate temperature during the MBE growth of GaN on sapphire. The lower curve shows the temperature as measured using traditional pyrometry while the upper curve shows the temperature after compensation by the reflectometry system.

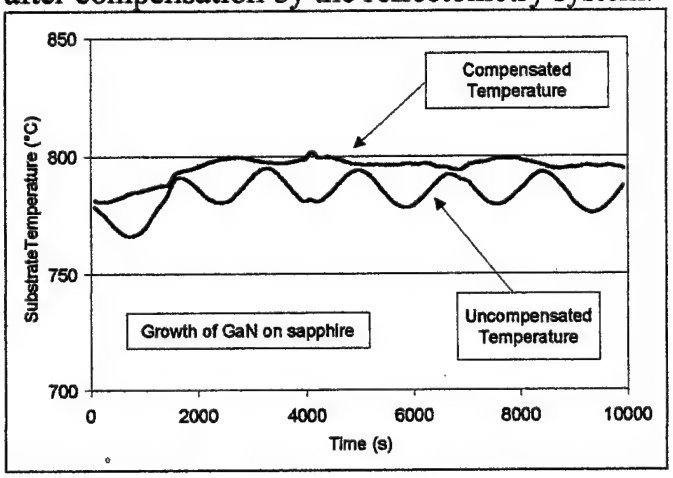

These new features of the In-Situ 4000 Process Monitor now allow accurate pyrometry to be performed in an MBE or MOCVD system.

In addition to accurate pyrometry, the reflectometer measures specular reflectance at two wavelengths: 950 nm and 470 nm. Reflectometry is obtained in real-time during deposition so that films which have differing index of refraction from the substrate produce reflectance oscillations in time. These reflectance oscillations can be analyzed in real-time to provide both film thickness and film index of refraction. The In-Situ 4000 has powerful analysis algorithms which can provide accurate growth rate, thickness, and index information. This valuable information can even be fed back to the growth system controller to achieve layer thickness precision improvements over traditional open-loop timed deposition control. The best growth rate and index of refraction measurements are obtained with films of at least $\lambda/4$ in thickness where λ is the reflectometer measurement wavelength (i.e. 950 nm or 470 nm).

The reflectometer uses two LEDs housed in the optical head to illuminate the wafer through the vacuum viewport window and detects the light with the same

optical system as the pyrometry. Thus the system need only use a single, normal incidence viewport which is provided in many vacuum systems. The viewport must be large enough to allow room for both the illumination light to enter and the reflected and pyrometric radiated light to exit the chamber. The In-Situ 4000 requires a 2.75 inch Conflat viewport or larger to accomplish this measurement. Another requirement is that the viewport window be located at normal incidence to the substrate so that the illumination beam be specularly reflected back to the instrument. This places some limits on the substrate holders which need to maintain normal incidence alignment during use and especially during wafer rotation. The In-Situ 4000 system has special software features which can allow the measurement to function well even if the substrate tilts strongly during wafer rotation.

The In-Situ 4000 Process Monitor provides the MBE or MOCVD user with a complete tool for obtaining in real-time the two most important process parameters in film growth: temperature and thickness. The system uses only a single viewport window at normal incidence and is specifically designed for MBE and MOCVD processes.

III. Growth Process Research Results

1. Ga_2 dimer spectroscopic analysis

In previous experiments in which the ULTRA sensor was used to detect the output of the Ga oven source, a small amount of Ga_2 was seen in the time-of-flight mass spectra. Thermodynamically, there should have been much less Ga_2 than was seen. This led to the conclusion that the ionization of Ga_2 molecules might involve a resonant excitation at 355 nm. First, it was determined that the Ga_2 ions were the result of multiphoton ionization by the scattered 355 nm laser light introduced into the chamber during the frequency tripling process to make 118 nm in Xe and Ar gases. The 355 nm photons were also responsible for some multiphoton signal of Ga atoms. Figure III.1 shows a 3000 laser pulse summation average of the mass spectrum of the Ga source beam. The three isotopes of $Ga_2$are clearly mass resolved at 138, 140, and 142 amu. The amount of Ga_2 that is ionized by 355 nm laser light is approximately 0.3 per cent of the amount of Ga atoms ionized by the 355 nm photons with no 118 nm light present. Next, the spectroscopy of Ga_2 was further examined using a dye laser to scan laser wavelengths from 355 to 335 nm. However, the results showed that the number of Ga_2 ions produced was unchanging over these wavelengths at laser powers of 3 mJ/pulse and laser

linewidths of 1 cm^{-1}. Future experiments are planned to further investigate the spectroscopy of Ga_2 using higher resolution,

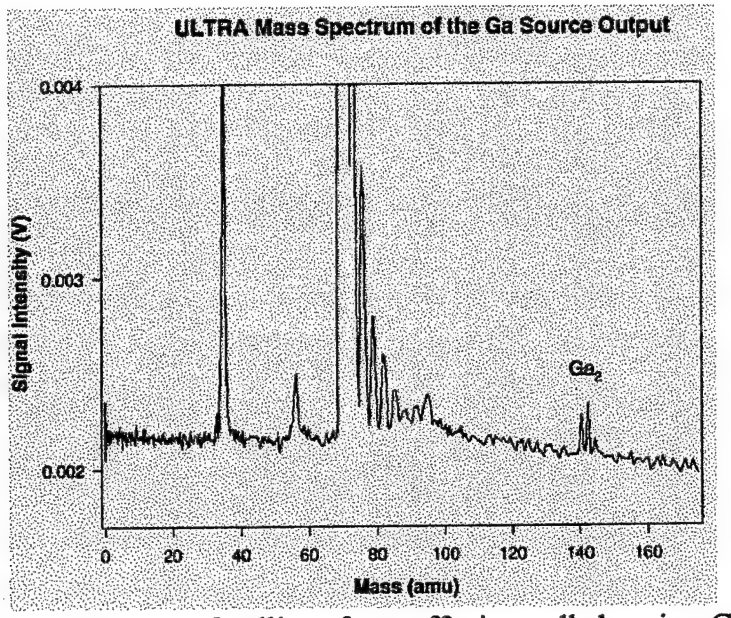

Figure III.1. Mass spectrum of gallium from effusion cell showing Ga2 dimer in the flux.

The spectroscopy of Ga_2 was further examined using a dye laser to scan laser wavelengths from 355 to 335 nm at higher resolution. However, the results showed that the number of Ga_2 ions produced was unchanging over these wavelengths at laser powers of 1 mJ/pulse and laser linewidths of 0. 1 cm^{-1}. Since the Ga_2 is at a high temperature, the density of states appears to be too high to resolve the spectra at this resolution. We tried to scan the region of the spectrum around 350 nm and do some spectroscopy on this species. The scanning scheme was to use 1 + 1 REMPI (single color) with TOFMS detection to obtain the absorption spectrum for Ga, in this spectra region. To do this we used a DCR-2A ND:YAG laser to pump (532 nm) a PDL-2 dye laser, followed by a WEX-1 frequency doubler. While a continuous ionization signal was observed, no spectral features could be detected. Subsequent modeling of the expected Ga_2 transition showed that the spectral congestion of the molecules from the high temperature effusion source was too great to be resolved. However, the multiphoton transition could be used in future investigations for Ga_2 species that might be produced during growth.

2.As_4 sticking probability on GaAs(100)

Data analysis of the sticking probability of As+ on the GaAs(100) surface was

concluded. Figure III.2 displays the sticking for As_4 and total arsenic species as a function of gallium flux to the surface. In both traces, the wafer is held at a constant surface temperature and at a constant arsenic incident flux. For the data presented in panel (a), the surface temperature is 855 °K, the incident As+ flux is 0.32 ML/s and the incident Ga flux ranges from 0.05 to 0.65 ML/s. For the data presented in panel (b), the substrate temperature is 873 °K, the incident As_4 flux is 0. 107 ML As atom/s, and the Ga flux ranges from 0.01 to 0.42 ML/s. The widely-accepted value of 0.5 for the maximum sticking probability of As_4 was measured only under growth conditions in which Ga islands were present on the surface (panel (b)). Under good growth conditions in which RHEED oscillations were observed (panel(a)), the sticking of As_4 was seen to exceed 0.5, reaching 0.92 at high incident gallium fluxes and low substrate temperatures.

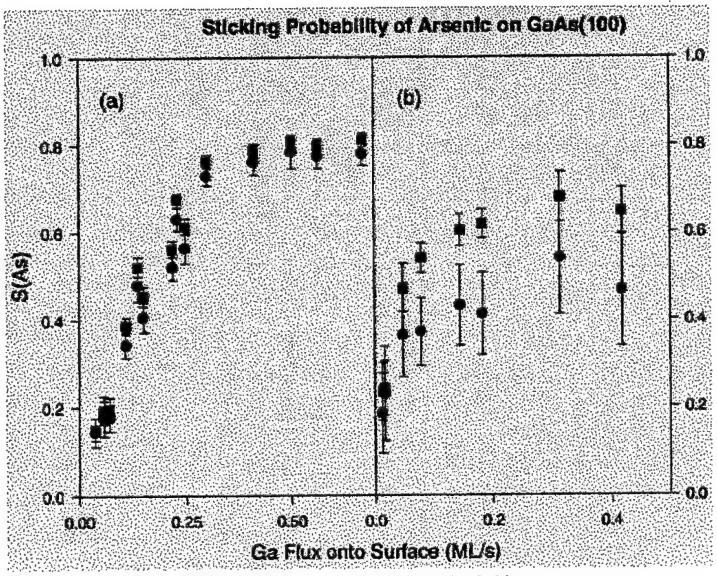

Figure III.2. Sticking probability of As on GaAs(100)

3.Desorption kinetics of arsenic from Si(100)

Further analysis of the desorption kinetics of arsenic species from Si(100) yielded the activation energy and pre-exponential for desorption of As atoms from Si(100) as well as insight concerning the desorption of As_2 from Si(100). The effects of incident As_4 flux on the amount of desorbing As atoms and As_2 are shown in Fig. III.3. The amount of As atoms desorbing from the Si surface saturates at the highest fluxes, indicating that atoms occupy limited sites on the Si surface, such as defects or steps. The real-time kinetic data revealed an activation energy of 1.64 ± 0.05 eV and a pre-exponential factor of $(8 \pm 3) \times 10^7\ S^{-1}$ for the desorption of As

atoms from these limited sites on the surface. The desorption kinetics of As_2 were found to be complicated by the existence of two different types of surface reconstructions of the As_2 rows on the surface as well as the decrease in the surface coverage of As_2 with increasing Si surface temperature. Further, the near linear dependence of the scattered As_2 signal with increasing As_4 incident flux indicates that at the highest substrate temperatures, the desorption of As_2 is fast and that the As_4 is catalytically cracked to As_2.

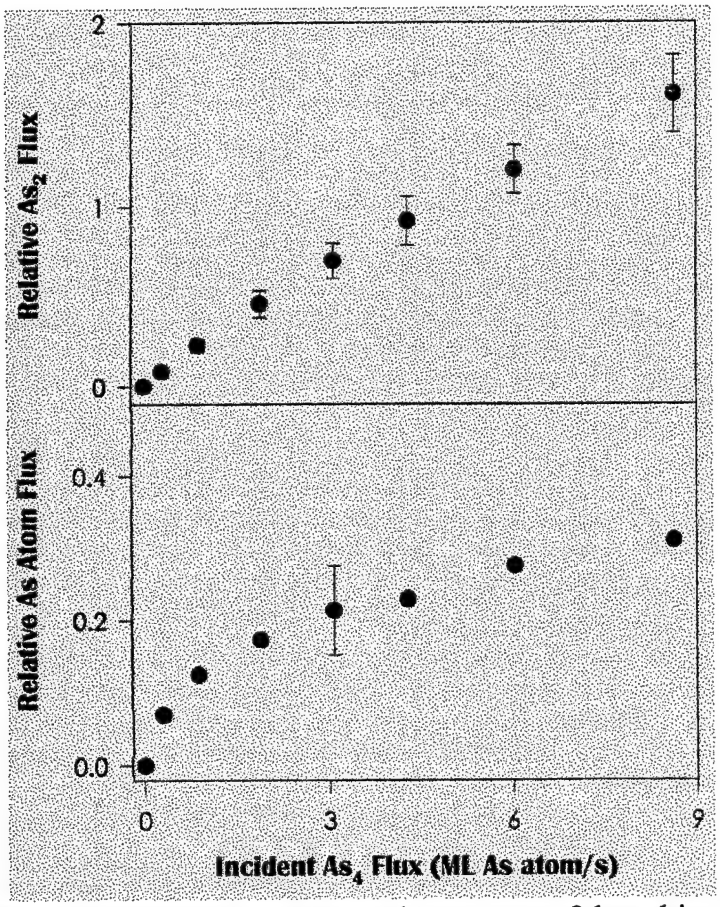

Figure III.3. Effects of incident As_4 flux on the amount of desorbing As atoms and As_2 dimers.

4. Surfactant enhanced epitaxy of Ge on Si(100)

Progress has been made extending previous studies on the surfactant enhanced epitaxy of germanium on Si(1 00) using arsenic as the surfactant. The evolution of arsenic dimers from the surface during germanium growth has been observed. Preliminary experiments have been carried out to monitor the As_4 and As_2 signals during germanium growth as a function of germanium flux to the surface. These preliminary results indicate that the number of dimers evolving from the surface

increases as the germanium flux to the surface is increased. An initial measurement also suggests that the amount of arsenic evolving from the surface increases as the substrate temperature is increased. Further experiments are in progress to quantify the change in the arsenic tetramer and dimer desorption as a function of germanium flux and substrate temperature.

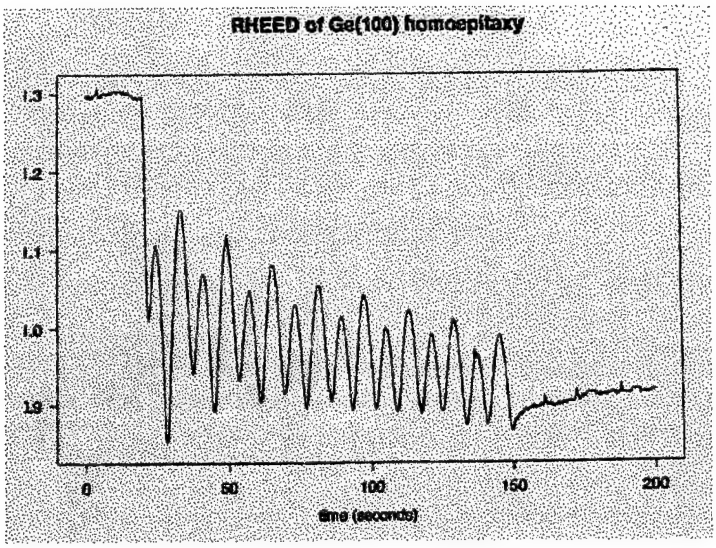

Figure III.4. RHEED oscillations during Ge homoepitaxy.

In previous studies, oscillations in the RHEED specular beam intensity during germanium epitaxial growth on Ge(100) were observed, Figure III.4. These oscillations showed alternations in intensity, with one strong oscillation followed by a weak one. This same behavior has been observed previously by another group in the epitaxial growth of silicon on Si(100) under conditions where the dimer rows on the substrate were all running in the same direction *(ie.* the only steps were bilayer high steps). The alternation in intensity from one oscillation to the next is observed because from one layer to the next the surface structure will change 1x2 or vice versa, with the direction of the dimer rows alternating from one layer to the next. The ability to observe this alternation in the oscillation intensity seems to depend critically on the incident angle as well as the incident direction of the electron beam. It seems reasonable that the RHEED oscillations observed for the epitaxial growth of germanium on Ge(100) can be attributed to the same kind of phenomenon. We intend to use these oscillations in the RHEED intensity to calibrate the flux of germanium to the surface during our surfactant enhanced epitaxy studies. In an attempt to elucidate the proper conditions (such as sample position, and Ge flux) for layer by layer growth of Ge, we have begun an investigation of Ge growth on Ge(100). This will hopefully help us to identify the proper conditions under which to attempt the growth of Ge on Si(100). These studies can also be used to calibrate the flux of germanium coming from the oven.

By monitoring the period of the RHEED specular beam intensity oscillations as a function of oven temperature, the flux for different oven settings will be obtained.

Progress has also included continuation of the studies of surfactant enhanced epitaxy of germanium on Si(100) by monitoring the intensity of the specular beam of the RHEED diffraction pattern during growth of Ge on Si(100) both with and without the presence of an arsenic flux. Over a wide range of surface temperatures and Ge fluxes we have been able to observe at most three oscillations in the RHEED intensity. We do however, see a dramatic decrease in the intensity of the RHEED pattern after the Ge oven is open and growth has begun. These results suggest that under the current experimental conditions, the growth is not in a strictly layer by layer fashion, but the preferred growth mode is either islanding, or layer by layer growth initially followed by islanding after a few layers.

We have also performed time resolved measurements of the scattered As_2 and As_4 during growth runs of Ge on Si(l00) with a flux of As_4 as a surfactant. In these experiments, the Si(100) sample was continuously bathed in an As_4 flux and growth of Ge is initiated and terminated by opening and closing a shutter on the Ge oven. When the Ge shutter is opened, an increase in the scattered As_2 flux and a corresponding decrease in the scattered As_4 flux are observed. After the Ge shutter is closed, the As_2 and As_4 signals do not recover to their initial levels. The magnitude of the change of the scattered As_2 and As_4 signals increases with increasing Ge flux. These results strongly suggest that islands are forming on the Si during growth. It is reasonable to expect that the scattered As_2 and As4 signals would change during growth since the sticking probability as well as adsorption and desorption energies for arsenic species on germanium may be different from those for arsenic species on silicon. If the change in scattered signal observed is due to the fact that the As_4 scatters from a germanium surface rather than from a silicon surface once growth has begun, we would expect that the change in the signal would saturate after the flux of germanium is sufficient to cover the surface with one monolayer of germanium. However, this is not what has been observed experimentally. The fact that the magnitude of the changes in the As_4 and As_2 signals continue to increase with increasing flux suggests that the surface area of germanium on the surface is continuing to increase. This could happen if the germanium is forming islands on the surface. This is consistent with the results of the RHEED experiments described above.

We investigated what parameters are important in controlling the growth mode in the Ge/Si(100) system and perform a systematic study of this process to determine energetics and growth mechanisms. This might also lead to the possibility of monitoring and controlling the formation of quantum dots *in situ* using RHEED and SPI-TOFMS. This can also be extended to the growth of silicon on Ge(100).

5.Application of ULTRA Metal-organic chemical vapor deposition

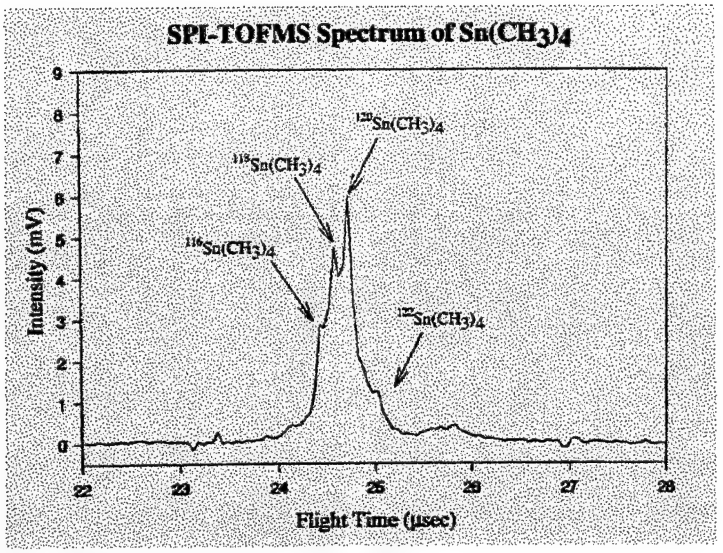

Figure III.5. SPI-TOFMS spectrum of $Sn(CH_3)_4$.

We recently demonstrated the ability to detect species used in metal organic chemical vapor deposition (MOCVD) as well as elemental sources used in MBE. Specifically, we have obtained a single photon ionization time of flight mass spectrum of tetramethyltin ($Sn(CH_3)_4$), Figure III.5. In addition, several other compounds commonly used in CVD processes have ionization potentials below the 10.5 eV photon energy available in our current ionization scheme. The range of accessible compounds could be extended by using a VUV lamp source for the ionization. For example, an argon lamp will give a photon energy of 11.8 eV. A sample of organo-metallic compounds which can be photoionized is given in Table III.1.

Ionization Potenials of Species of Interest in Chemical Vapor Deposition (CVD)	
Si	8.15
SiH_4	11.65
$(CH_3)_3Si$	9.8
Si_2H_6	9.7
Ge	7.9
GeH_4	11.33
$(CH_3)_3Ge$	9.33
$(CH_3)_3Al$	9.78
$(CH_3)_3Sb$	7.7
$(CH_3)_3Ga$	8.9
$(CH_3)_3Sn$	7.1
$(CH_3)_4Sn$	8.89
$(C_2H_5)_3Sb$	9.2

Table III.1. Ionization potentials of species of interest in Chemical Vapor Deposition (CVD).

6.Commercial prototype of ULTRA

A low cost, reliable noble gas discharge lamp has been developed for soft, VUV photoionization. This technique is highly selective for growth and dopant species flux detection. For example, soft VUV photoionization can be used to distinguish Si, mass 28, from a large background of N_2, also mass 28.

The working principle of a compact VUV photoionization TOF mass spectrometry sensor has been demonstrated. Unlike conventional photoionization TOF designs which require separate optical and flight tube vacuum ports, this sensor combines them together onto a single 4.5 " conflat flange. The design also allows for dual mode electron impact- or photo-ionization. Alternatively, the single port sensor can be used with more conventional photoionization techniques such as laser multi-photon ionization (MPI). Figure III.6 shows a photograph of commercial version of the ULTRA sensor being developed at SVTA.

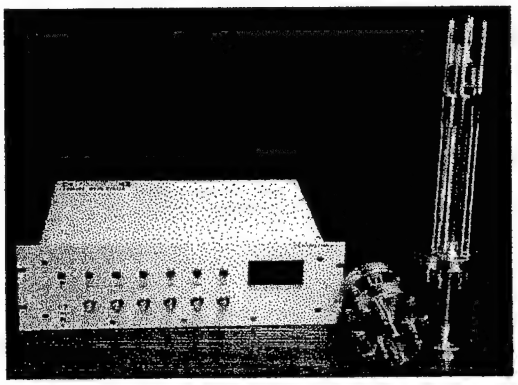

Figure III.6. Commercial prototype of ULTRA sensor.

7. Photoionization with microwave lamp

The commercial prototype of the ULTRA sensor has been tested in the SVTA laboratories. A test system consisting of a small, cryogenically pumped, multi-port vacuum system was assembled to test various the operation of the ULTRA sensor in various configurations. Both multiphoton laser ionization and single photon VUV photoionization configurations are possible. Figure III.7 shows the test configuration used for the study of single photon, VUV photoionization using resonant radiation from a micrwave discharge Krypton lamp.

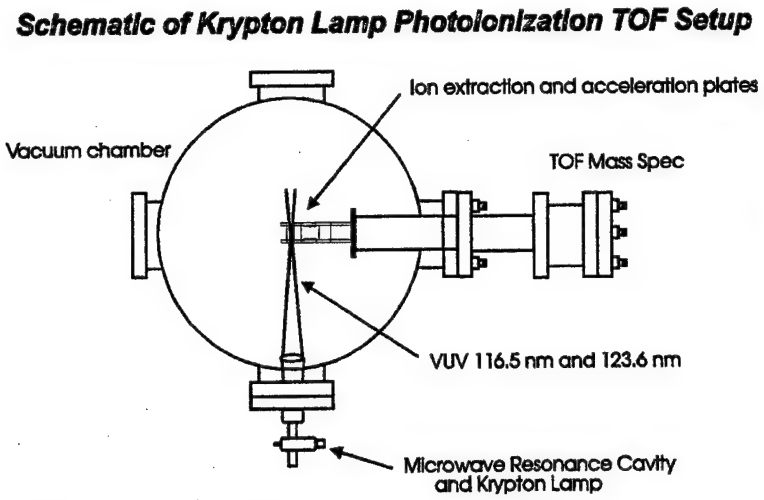

Figure III.7. Schematic of test system for microwave resonance lamd photoionization.

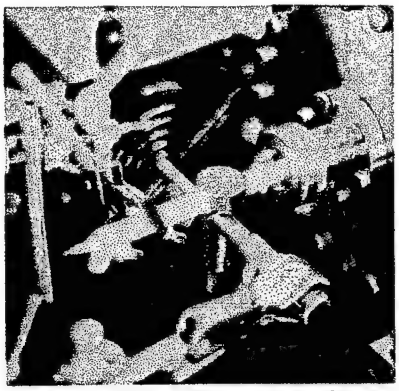

Figure III.8. Closeup of microwave resonance lamp.

Using this test setup for the prototype commercial ULTRA sensor, we have demonstrated the effectiveness of the microwave resonance lamp for single photon ionization. Shown in Figures III.9 and III.10 are examples of the mass spectra obtained for teramethyl silane (TMS) using this system.

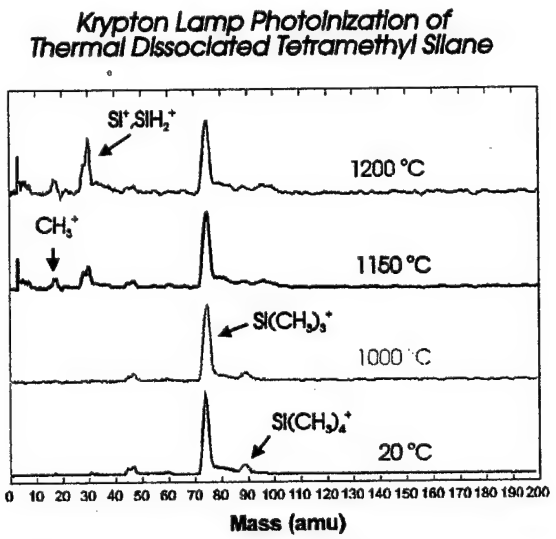

Figure III.9. Mass spectra for TMS using the prototype commercial ULTRA sensor

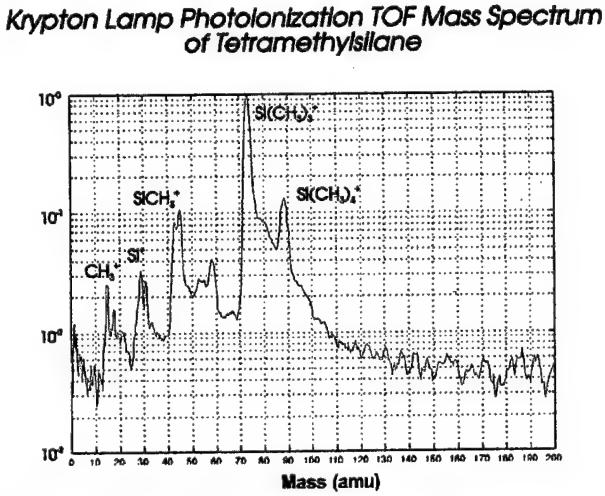

Figure III.10. TMS photoionization mass spectrum.

The advantage of going to resonant lamp ionization in the commercial ULTRA system versus generation of the 9th harmonic of Nd:YAG is in the reduction in cost and simplicity of operation. The lamp photoionization offers an order of

magnitude reduction in cost, from $100,000 for the laser system to ~$10,000 for the lamp.

8.Surfactant enhanced epitaxy of Ge on Si(100)

Progress has been in the studies of surfactant enhanced epitaxy of germanium on Si(100) by calibrating the flux of Ge from the Ge oven using RHEED oscillations, and by performing studies of the As_n desorption kinetics from Ge(100) and Si(100) under steady state conditions.

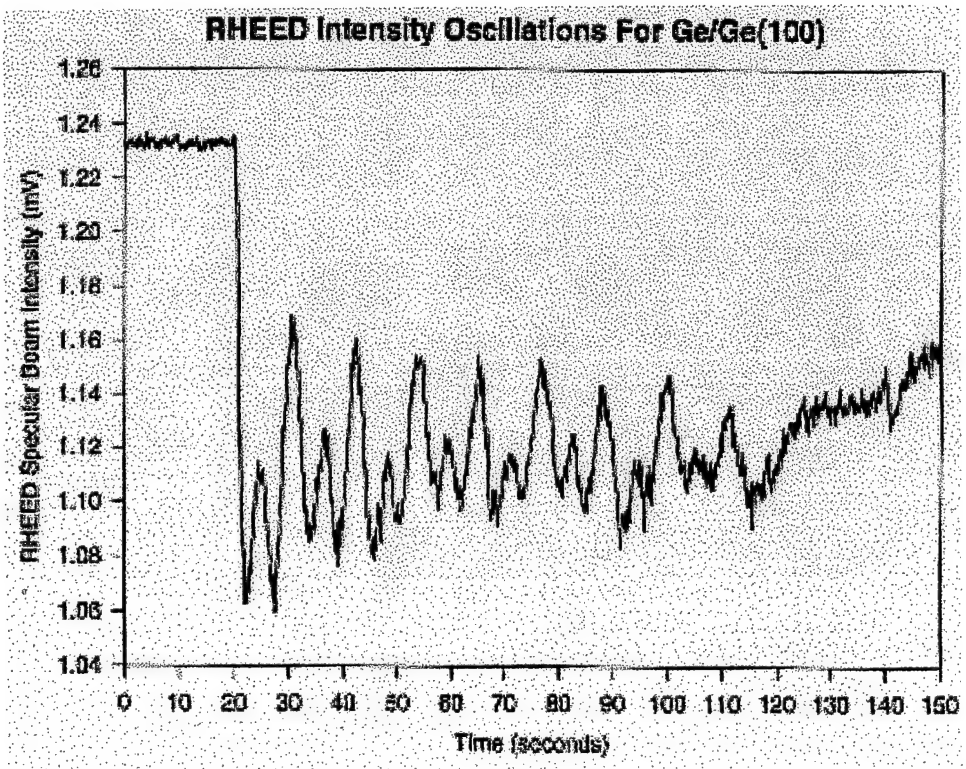

Figure III-11. First Oobservation of RHEED oscillation during the epitaxial growth of Ge on Ge.

The examination of the growth of Ge on Ge(100) was undertaken both to calibrate the Ge flux from the Ge oven and find reasonable conditions under which to attempt the Ge growth on Si(100) in the surfactant enhanced epitaxy studies. The RHEED specular beam signal for a growth run of Ge/Ge(100) is shown in Figure III.11. The surface temperature during this growth run was held at about 740 K, and the growth rate was -0.17 Monolayers/sec (determined from the RHEED oscillation period). The Ge oven temperature was held at 1290' C for this data run. It is interesting to note that the alternation in the intensity of these oscillations, from one to the next) has been seen on Si(lll), Ge(lll), and Si(100), but to our knowledge it has not been previously reported on Ge(100). The exact cause of the dual nature of these oscillations is currently under investigation. The growth rates presented here have assumed that each of these maxima in the RHEED oscillation

signal corresponds to the completion of one layer. To get a calibration of the flux of Ge from the oven, the same experiment was carried out at several different oven temperatures. The results are shown in Figure III.2, in which the growth rate from the RHEED oscillation period is plotted against Ge oven temperature. As expected, the growth rate is lowest at the lowest oven settings and increases with increasing oven temperature. Over the range of temperatures studied here, the growth rate seems reasonably linear with the oven temperature. These results can now be used as a calibration of the Ge flux in the surfactant enhanced epitaxy experiments.

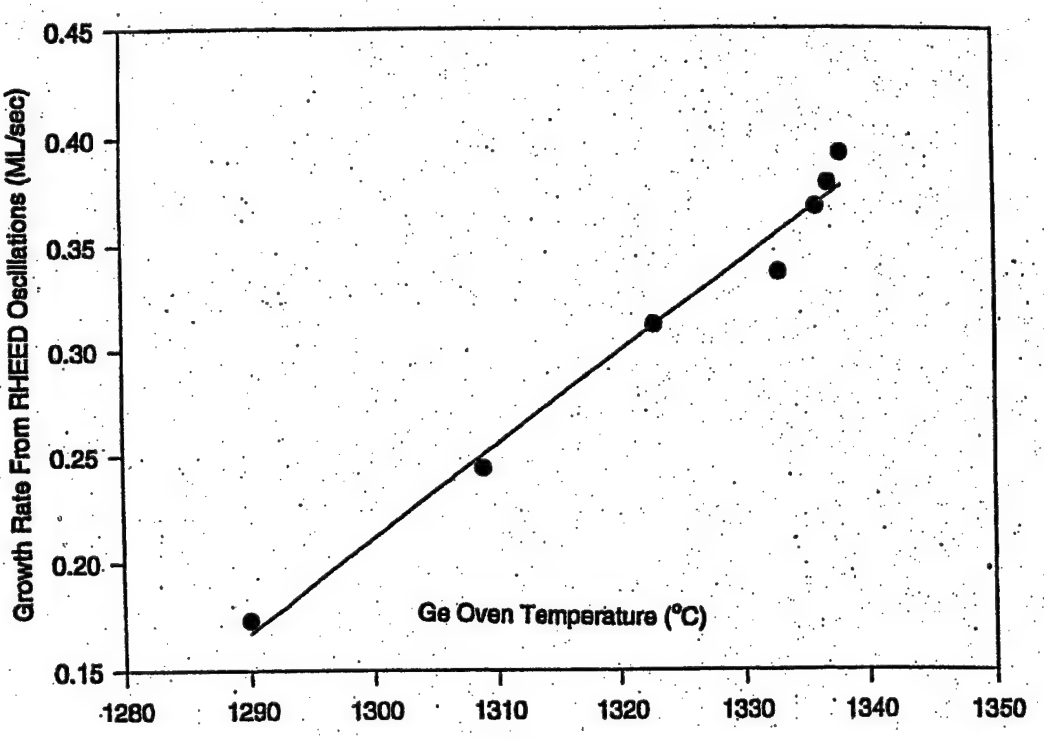

Figure III-12. Growth rate as function of the source temperature, calibrated with RHEED oscillation.

Experiments have also been performed on the desorption kinetics of different arsenic species from Ge(100) and Si(100) wafers. In these experiments, the wafer is held at a fixed temperature under an incident flux of As_4 and the relative intensities of the different arsenic species desorbing from the surface are determined. Figure III.3 shows the results of these experiments for a Ge(100) wafer and Figure III.4 shows the results of a similar experiment on a Si(100) substrate. The As_4 flux is approximately the same in both cases (As oven temperature ~335° C). At the lowest substrate temperatures studied, the predominant desorbing species is As_4. As the substrate temperature is raised, the amount of scattered As_4 decreases and the amount of As_2 increases. In the case of

the Ge(100) substrate, the amount of As_2 continues to increase from about 600 K to about 1000 K. In contrast, a broad plateau is seen in the As_2 desorption from Si(100). This had been observed in previous experiments, but so far has not been satisfactorily explained. By comparing the results from the Ge and Si experiments, we hope to determine the mechanism responsible for this unusual behavior. In addition to the As_4 and As_2 signals, at temperatures above about 1000 K, the evolution of As atoms from the surface is observed from both the Ge(100) and Si(100) substrates, and from the amount of As atoms evolved at different temperatures, an activation energy for desorption of As atom from both surfaces can be determined.

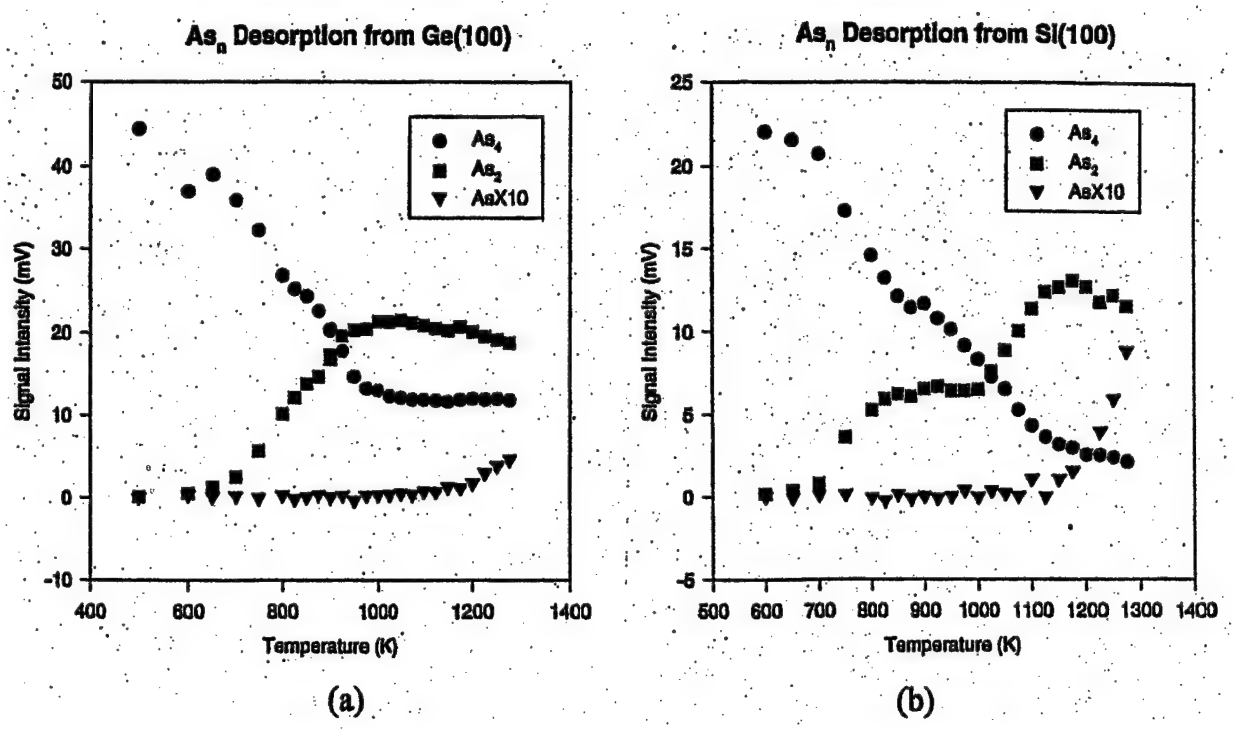

Figure III-13. (As_n desorption from Ge(100), compared to (b) that of from Si(100).

Initial experiments on the surfactant enhanced epitaxy of Ge/Si(100) have shown that As_2 is liberated from a Si(100) wafer bathed in an As_4 flux when the Ge shutter is opened and growth begins. This would tend to indicate a difference in energetics of adsorption or desorption of the arsenic species on Ge(100) and Si(100) and we hope to be able to answer this question with the As_n desorption studies. Having observed oscillations in the RHEED intensity during growth of Ge/Ge(100), experiments can now be performed, using similar conditions as a starting point, growing Ge on Si(100) to find the appropriate conditions for layer by layer growth in that system. Once the mechanisms for surfactant enhanced

epitaxy are understood, there is the possibility of controlling the growth mode of the film to yield structures such as quantum dots.

9.Arsenic desorption kinetics from Si(100) and Ge(100)

Further investigations of the desorption kinetics of different arsenic species from both the Si(100) and Ge(100) surfacesis useful to determine the mechanism giving rise to previously observed RHEED oscillations during the growth of Ge on Ge(100). Studies have also been carried out to study the formation of quantum dots in the Ge/Si(100) system.

By performing steady state measurements of the arsenic desorption from Si(100) and Ge(100) surfaces, a direct comparison of the energetics of these processes on the two different surfaces can be made, which is important in understanding the results from the surfactant enhanced epitaxy studies. Previously we have demonstrated that clear differences exist between the As_2 desorption signals on these two surfaces. Preliminary results suggest that the angular distribution of the scattered products may change with surface temperature and this could explain the observation of a plateau in the As_2 signal as a function of temperature in the desorption experiments on Si(100). A similar plateau is not observed in the case of Ge(100) experiments. This suggests that there may be two pathways for desorption of As2 which compete in the case of Si(100) but not in the case of Ge(100).

During the growth of Ge on Si(100), the Ge can only grow layer by layer for about 3-5 monolayers before the Ge starts to form islands on the surface. Surfactants such as arsenic have been shown to suppress this islanding transition, thereby changing the growth mode of the film from islanding to layer by layer. Experiments have been carried out to determine the effect of the introduction of a surfactant on the size and spatial distribution of islands formed in this system. Specifically, scanning electron microscopy (SEM) images have been obtained of Ge islands formed on Si(100) after deposition of -10 monolayers of Ge at a substrate temperature of 750 K, and it is confirmed that the resulting islands are ~50-100 mn in diameter. Samples have also been grown where a surfactant has been introduced before the growth of the Ge is started. By varying the arsenic deposition conditions, the initial concentration of the arsenic on the surface has been changed from -1 monolayer to less than 0.25 monolayers. It has been suggested that the surfactant provides nucleation sites for the formation of the islands, so if this is true we expect to observe a large change in the size and density of the islands formed as the initial arsenic concentration is changed. The surface temperature and Ge flux to the surface can also be varied to observe the effect of these parameters on the resulting film. Once the changes in the morphology of the flhns with different conditions are understood, it is hoped that the growth of these

quantum dots can be monitored using the single photon ionization time of flight mass spectrometer currently available in our system. This would allow for in situ monitoring and control of the formation of these quantum dots.

10.Germanium quantum dot formation

In previous experiments, it was shown that the desorbing As_2 and As_4 fluxes from a Si(100) wafer are altered significantly when the growth of germanium is initiated on this surface. Specifically, as germanium is deposited, the As_2 signal increases substantially and the As_4 signal shows a corresponding decrease. Once the germanium deposition is terminated by closing the shutter, the signals do not recover to the initial levels before the deposition of germanium. This is demonstrated in Figure III-14, where a Si(100) surface was held at a constant temperature while under a constant As_4 flux. The shutter on the germanium oven was opened at time t--20 seconds and closed at t--40 seconds. Notice the drop in the arsenic dimer signal and fact that the signals do not return to the original level upon closing the shutter. This points to dramatic differences in the desorption kinetics of As_2 from the germanium and silicon surfaces.

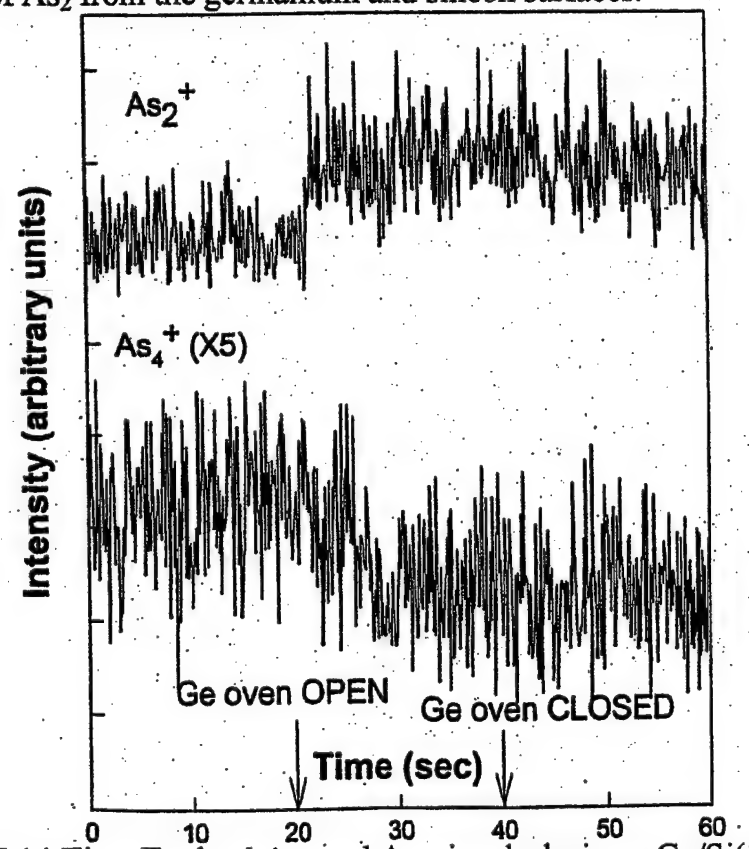

Figure III-14.Time Evolved As_4 and As_2 signals during a Ge/Si(100) growth run.

Experiments have been performed to investigate the differences in the desorption kinetics of different arsenic species from Ge(l00) and Si(l00) to shed light on the surfactant enhanced epitaxy results presented above. In the case of Si(100) a plateau is observed in the As_2 signal as a function of temperature. In the range from 800-1000 K the dimer signal level is fairly constant and then begins to increase again at temperatures above 1000 K. Experiments have been performed to investigate this plateau in As_2 evolution from the Si(l00) surface as a function of temperature. There is no such plateau observed in the case of As_2 desorption from Ge(l00). One possible explanation is a change in the angular distribution for desorption from silicon and germanium. The dependence of the As_2 signal on temperature at several different laser probe positions has been investigated for the case of the Ge(100) surface. By changing the laser probe position in this system, different parts of the scattered angular distribution of the products can be intersected. In the case of the Ge(100) surface, the shape of the As_2 desorption curve does not change significantly by changing the probe position, as demonstrated in Figure III-15. In the case of Ge(100), the signal we observe doesn't depend strongly on the portion of the angular distribution we intersect, suggesting that the scattered flux of As_2 is fairly isotropic over the temperature range studied here. Experiments are currently underway to investigate the AS2 desorption from Si(100) at different probe positions. This should elucidate whether the plateau we observe in the dimer desorption signal from Si(l00) is due to two different processes occurring with different angular distributions.

Work on the effect of arsenic on the growth of islands of germanium on Si(100) was performed to investigate the effect of initial arsenic coverage on the size and density distributions of islands formed. This morphology of the films has been studied using atomic force microscopy (AFM). With no initial arsenic on the surface, after depositing about 3-6 ML, the streaky RHEED pattern turns spotty, indicating the transition to island growth, as many previous studies have shown. AFM images of the surface after growth show many large (-50-100) islands on the surface. These islands grow larger with increasing germanium coverage. Samples have been grown at several different germanium coverages with a range of different initial arsenic coverages to study the effect of arsenic on the size and density distributions of the resulting films. AFM images show that as the initial arsenic concentration is increased, the islands formed are smaller and more densely packed. This is demonstrated clearly in Figure III-16 for a germanium coverage of 25-30 ML. In all of the large scale AFM images of these germanium films, we observed the presence of a number of larger islands that appear to be a collection of many smaller islands. Much work has been done in an attempt to discover the origin of these features. Work by the Krishnamurthy group suggests that these

large islands could be due to small silicon carbide impurities present on the wafer before growth, which act as nucleation sites for the growth of islands. While typically no carbon is seen in the Auger electron spectra of these samples before the growth, it is still possible that there are small silicon carbide particles present at a low enough density that we can not detect them with this technique. One possibility to eliminate the effect of these nucleation sites on the subsequent growth is to effectively bury them under a thick buffer layer of silicon.

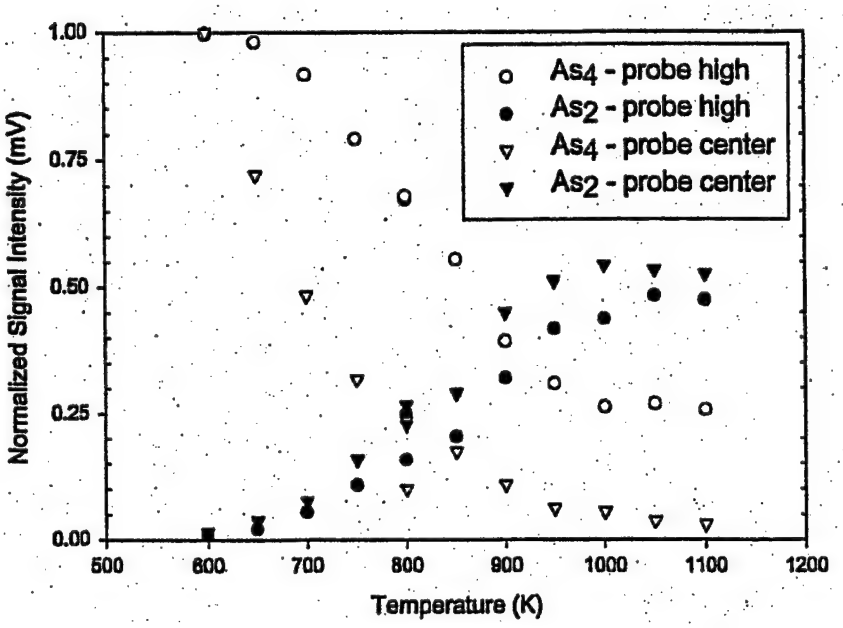

Figure III-15.Desorption As_n flux distributions as measured by different probe positions.

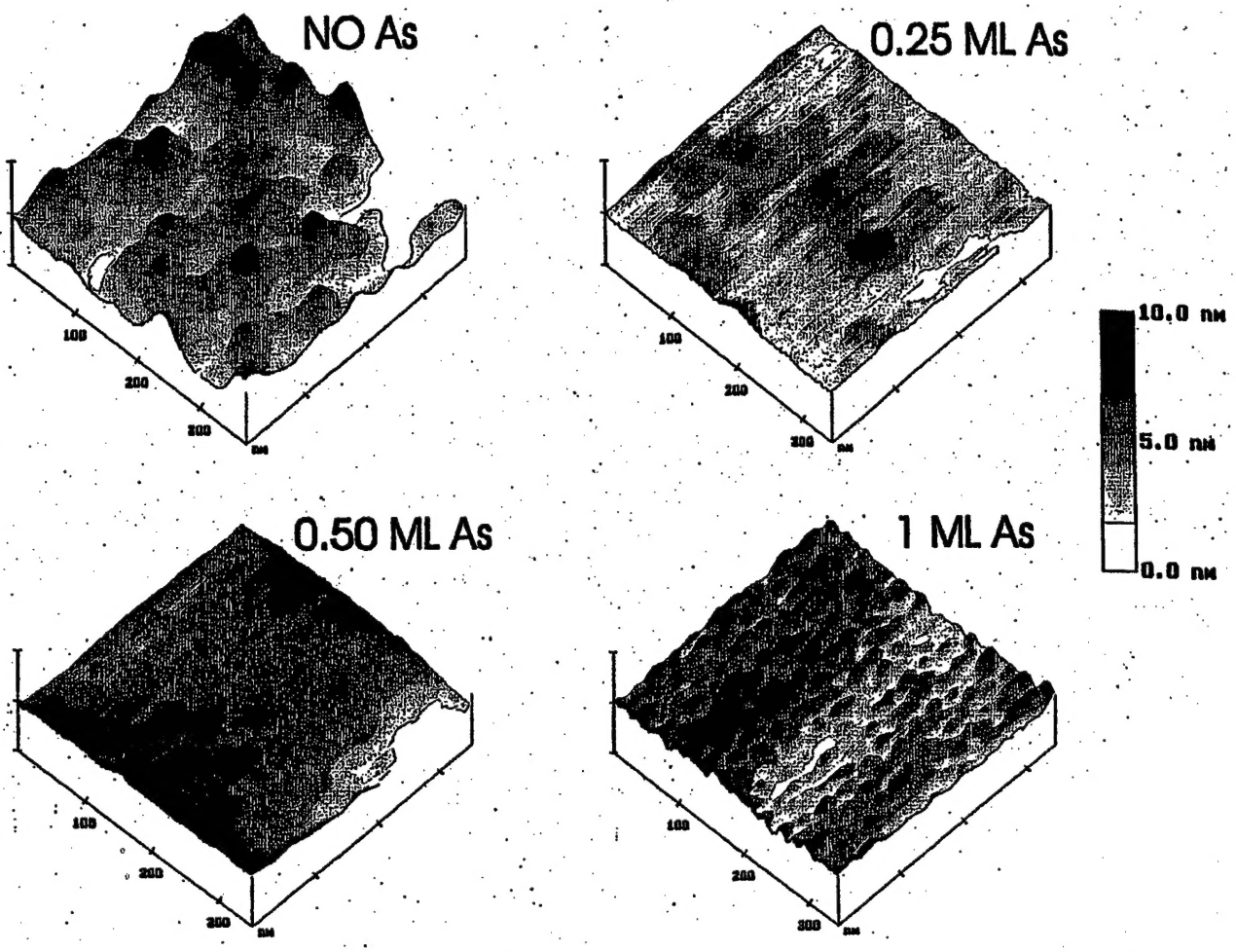

Figure III-16. Atomic Force Microscope (AFM) of Ge quantum dots grown under differnt As coverage.

In an attempt to ensure that the initial surface that we are growing on is as flat and defect free as possible, we have recently added an electron beam source of silicon to the chamber. This source is now positioned in the oven region, after initial testing, and is ready to be used to grow buffer layers of silicon on the Si(I 00) wafers before the germanium growth experiments begin. The flux of silicon from the oven can determined by monitoring the period of the RHEED oscillations during growth.

Several different aspects of the surfactant enhanced epitaxy of germanium on Si(100) have been investigated in this work. They include the time dependent evolution of arsenic species from the surface during, growth of germanium on Si(100), the desorption kinetics of different arsenic species from Si(100) and

Ge(100), the use of surfactants to control the size and density distributions of islands formed during growth of germanium on Si(100).

Formation of the SiGe islands are highly sensitive to the substrate temperature. Working with Professor M. Krishnmaurphy of the Michigan Technology University, island formation of 4-5 nm thick SiGe films may be illustrated by the surface morphology evolution at various temperatures. At 450°C the surface shows no well-defined islands but has surface roughness of the order of ~1 nm. Figure (a)-(c) below show islands formed at 500, 700, and 800 °C, respectively. Note that the islands are clearly defined, and appear as compact square-based prisms. Interestingly though there is no clear island formation visible at the substrate temperature of 600°C under otherwise very similar conditions. More detailed experiments determined that this behavior is reproducible and is due to a complex mechanism of segregation and inter-diffusion effects. These studies were carried out with SiGe films of very low concentration of Ge (about 1%). The coherent island formation of even low-mismatched SiGe films are shown to vary with alloy composition. This further highlights the importance of close flux and temperature control in the nano-structure fabrication process.

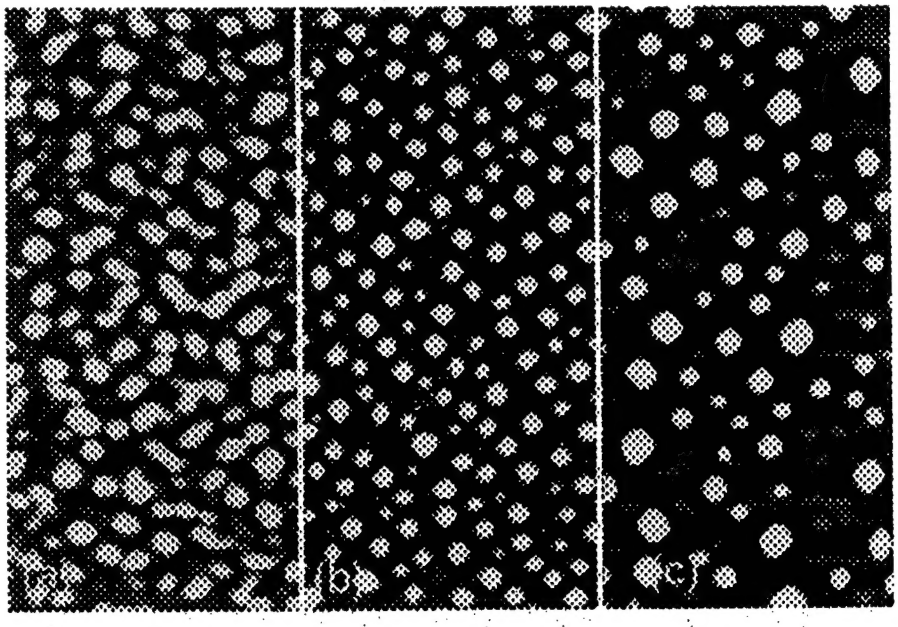

(a) (b) (c)

Figure III-17. AFM images of 3D island formation at various substrate temperatures. (a) 500°C, 0.5μm x 1μm scan, (b) 700°C, 1.25μm x 2.5μm, and (c) 800°C, 1.25μm x 2.5 μm. There appeared no island formation at 600°C.

IV. SUMMARY ACCOMPLISHMENTS

This three year program has demonstrated the applicability and effectiveness of the ULTRA sensor as a monitor for MBE growth processes. Work has been carried out using the combination of the various sensor techniques to demonstrate thickness and composition control for nanoscale electronic devices. The Ultra tool has been applied in SiGe heteroepitaxy where key understanding has been achieved of temperature, flux, and surfactant effects that are relevant to nanoscale device fabrication. Several of the techniques developed under this program is being commercialized as process control monitoring products.

The highlights of this program are the following.

Optimized Ultra Tool By implementation of high quality laser and optics

- Factor of five increase in 9th harmonic (118 nm) generation
- Low cost atomic resonance lamps examined as alternative VUV source

- Optimization of Time-of-Flight (TOF) hardware
- Quantification of the detection efficiency of flux species

Implemented Sensor Suite for MBE Process

- Implementation of prototype ULTRA on deposition system
- Development of optical scattering and advanced pyrometry tools
- Interface-capability to process automation software control

DevelopedFabrication Process of Nano-structures

- Surface dynamics study of GaAs homoepitaxy
- InAs quantum dot growth on GaAs
- SiGe nano-strucutre fabrication as function of flux and temperature
- Investigation of the effect of surfactants

Commercialization of in situ monitoring products

- Pyrometry interferometer as model IS 4000
- Improved RHEED image analysis
- Low cost Ultra instrument utilizing lamp ionization